ARC Far Side Impact Collaborative Research Program – Task 5: Test Procedures and Injury Criteria

Tom Gibson
Human Impact Engineering

Richard M. Morgan
George Washington University

Andrew Kemper and Stefan Duma
Virginia Tech – Wake Forest
Center for Injury Biomechanics

JANUARY 2007

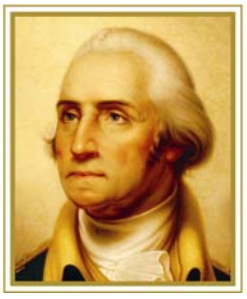

THE GEORGE WASHINGTON UNIVERSITY
WASHINGTON DC

Table of Contents

Table of Figures

Table of Tables

1 INTRODUCTION

The aim of Task 5 – Test Procedures and Injury Criteria of the ARC Far Side Collaborative Research Program, MUARC (2003) - was to conduct a test program and injury criteria investigation to identify or develop risk functions for far side occupants involved in side impact collisions. The task objectives were as follows:

- To quantify injuries and identify mechanisms of injury in far side impact;
- To identify attributes that may affect injury risk;
- To help develop probability of trauma functions for measuring injury risk in this crash mode. At a minimum the functions were to include:
  1. a head injury criteria,
  2. a trauma metric for hard-structure neck injury,
  3. the best construction of a metric for carotid artery dissection, and
  4. an abdominal criteria for far-side impact.
- To help develop and quantify injury risk parameters (for both soft tissue and bone fracture) for use in assessment of potential safety countermeasures.

This document reports on the work carried out in part fulfillment of the requirements for Task 5, the investigation of injury criteria suitable for use with occupants in far side impacts. The report includes both the identification of existing risk functions and the development of new functions as appropriate for use in dummy development, establishing injury criteria, and in modeling and countermeasure programs.

2 INJURY IN FAR SIDE IMPACTS

1.1 Injury Priorities

In a recent paper, Gabler et al. (2005a) evaluated the risk of side impact injury for far side impact. This analysis was based on NASS/CDS 1993-2002 and examined injury outcomes for over 4500 three-point belted occupants of cars, light trucks and vans involved in a far side impact. This analysis is used in this report to characterise the impact conditions which lead to far side injury and to set the priorities for the development of a comprehensive set of injury risk functions. In a second paper, Gabler et al. (2005b) compared the situation in Australia and the USA. The injury priorities for the body regions as a result of far-side impacts from Gabler et al. (2005b) are shown in Figure 1 and listed in Table 1 for both the USA and Australia. The injured body regions with the highest priority in terms of HARM were found to be the upper extremities, the head, the lower extremities followed by the spine, face, chest and abdomen.

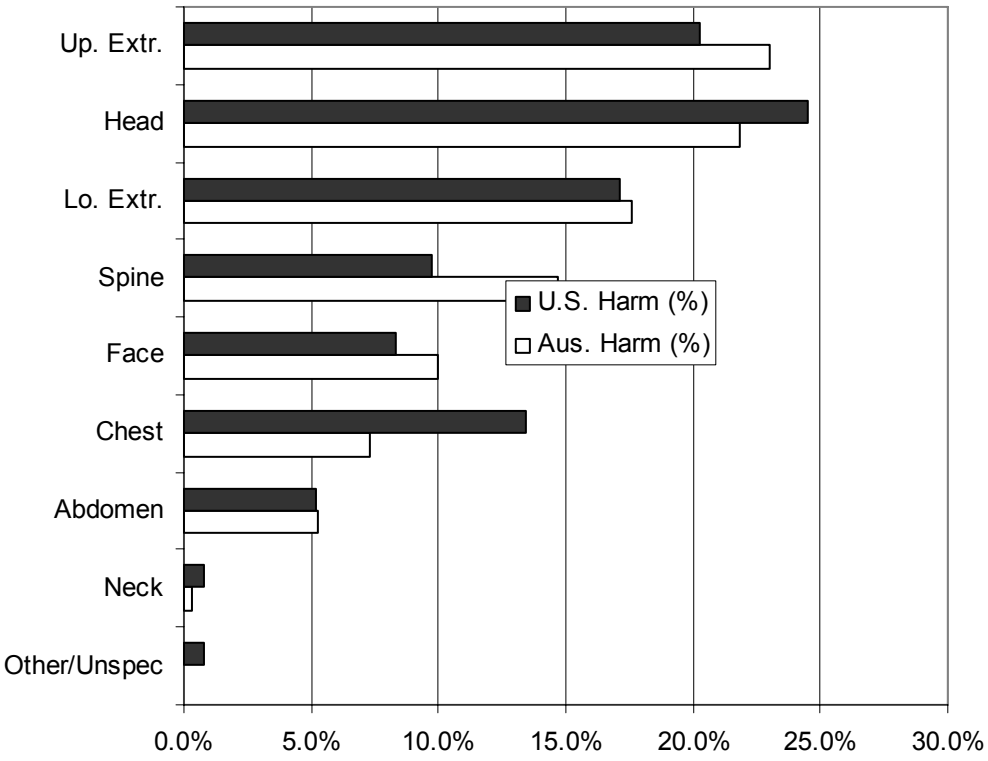

Figure 1 Injury priorities of body regions as a result of far-side impacts from Gabler et al. (2005b)

Table 1 Injury priorities of body regions as a result of far-side impacts based on Gabler et al. (2005b)

PRIORITY	BODY REGION	% HARM	
		AUS	USA
1	UPPER EXTR	23.0	20.3
2	HEAD	21.8	24.5
3	LOWER EXTR	17.6	17.1
4	SPINE	14.7	9.7
5	FACE	10.0	8.3
6	THX (+HLSK)	7.3	13.4
7	ABD (-LSK)	6.3	5.2
8	NECK	0.3	0.8
9	OTHER	0.0	0.8

In Figure 2 is presented the distribution of injuries by the principal direction of force (PDOF) in the crash, where zero degrees is the front of the car. The testing and modeling must be capable of reproducing the impacts between 30° and 90°. A PDOF of 60°was found to be most injurious.

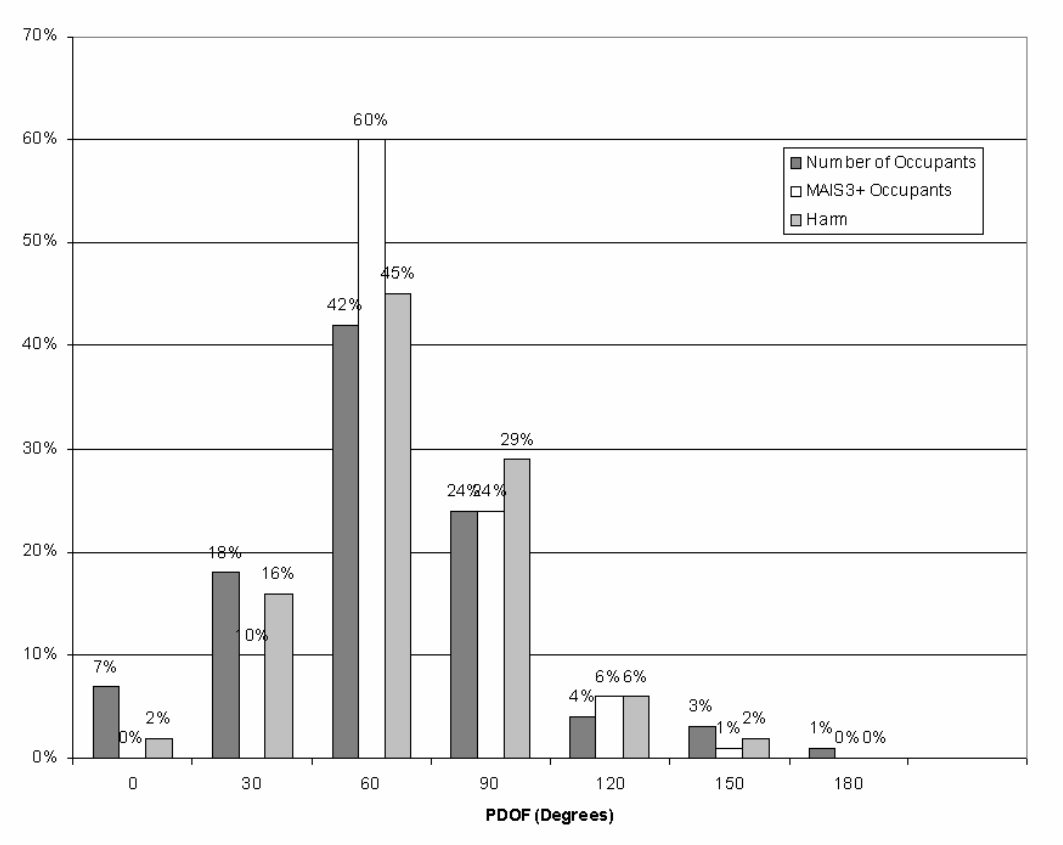

Figure 2 Injury by PDOF as a result of far side impacts from Gabler et al. (2005a)

The most common vehicle interior contacts found by these researchers for the occupants in far side impacts are listed in Table 2.

Table 2 AIS 3+ injuries to belted front seat occupants in far side impact by injuring contacts, NASS/CDS 1988-1998 Gabler et al.

INJURY SOURCE	ALL OCCUPANTS (%)	DRIVERS (%)	RF PASSENGERS (%)
R/S Interior	26.7	30.5	0
Seatbelt	20.8	22.6	8.5
Roof	12.2	13.1	5.9
All other	8.7	8.2	12.4
Seat	7.5	3.5	35.4
L/S interior	7.2	8	1.7
Non contact	6.4	6	9
Dashboard	5.2	4.3	11.4
Other occupant	2.9	1.4	13.2
Steering system	2.4	2.4	2.5

These are the source of injury and are important both in getting the injury risk function correct and in the design of counter-measures. The contact will be dealt with in more detail in the following section along with the body regions injured.

Based on the far side accident data in Gibson et al. (2003), the injury priorities for far side collisions by were assessed by body region total Harm. The priority for the body regions with the three highest priority AIS injury severities are listed Table 3. These priorities guided the risk function development.

Table 3 The injury priorities for far side are listed, based on the individual body region Harm along with the three highest priority AIS injury severities for each region (the darker the shading the higher priority), Gibson et al. (2003).

Body Region	AIS 1	AIS 2	AIS 3	AIS 4	AIS 5	AIS 6
Upper Extremities						
Head						
Lower Extremities						
Spine						
Face						
Thorax (inc HLSK)						
Abdomen (-LSK)						
Neck						
Shoulder						
Pelvis						

2.1 Specific Injuries in Far Side Crashes

A brief review was undertaken of the actual injuries suffered in be belted drivers in far side impacts in NASS for the years 2002 (n=27) and 2003 (n=32), Digges (2006). The aim of this review was to assist in understanding the specific injury types and the typical contacts causing these injuries. The injury types by body region for these belted drivers are given in Figure 3 for the upper and lower extremities and pelvis, Figure 4 for the head, Figure 5 for the neck and spine, Figure 6 for the thorax and Figure 7 for the abdomen.

Figure 3 Injury to the upper and lower extremities and pelvis of belted drivers in far side impacts in NASS for the years 2002 (n=27) and 2003 (n=32).

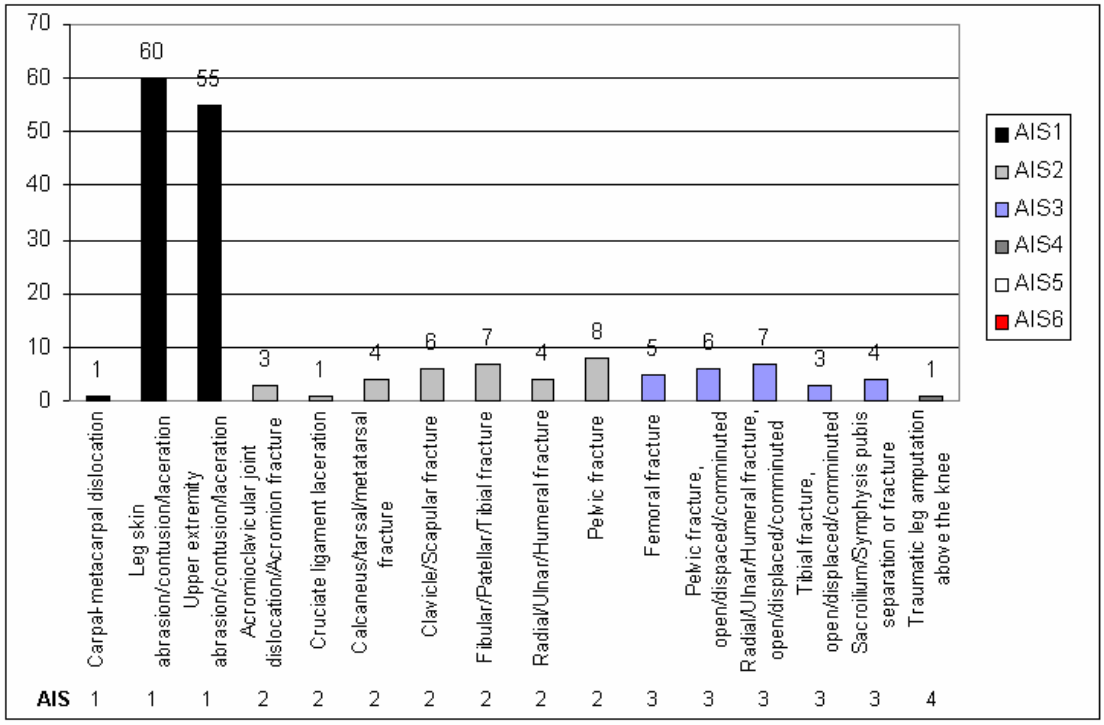

Figure 4 Injury to the head and face of belted drivers in far side impacts in NASS for the years 2002 (n=27) and 2003 (n=32).

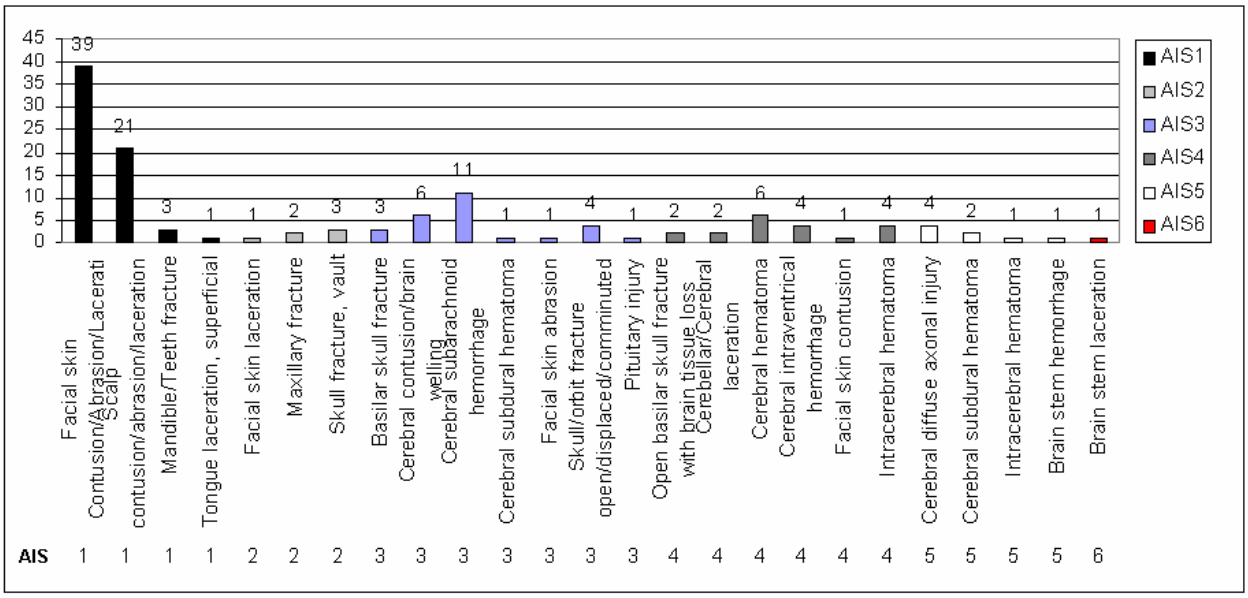

Figure 5 Injury to the neck and spine, belted drivers in far side impacts in NASS for the years 2002 (n=27) and 2003 (n=32).

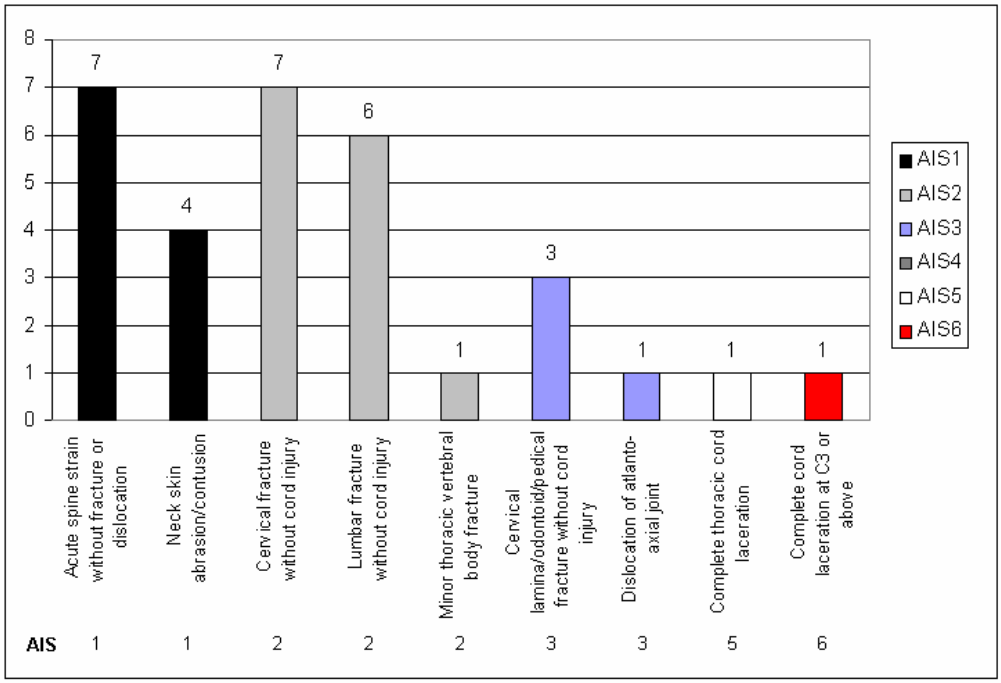

Figure 6 Injury to the thorax, belted drivers in far side impacts in NASS for the years 2002 (n=27) and 2003 (n=32).

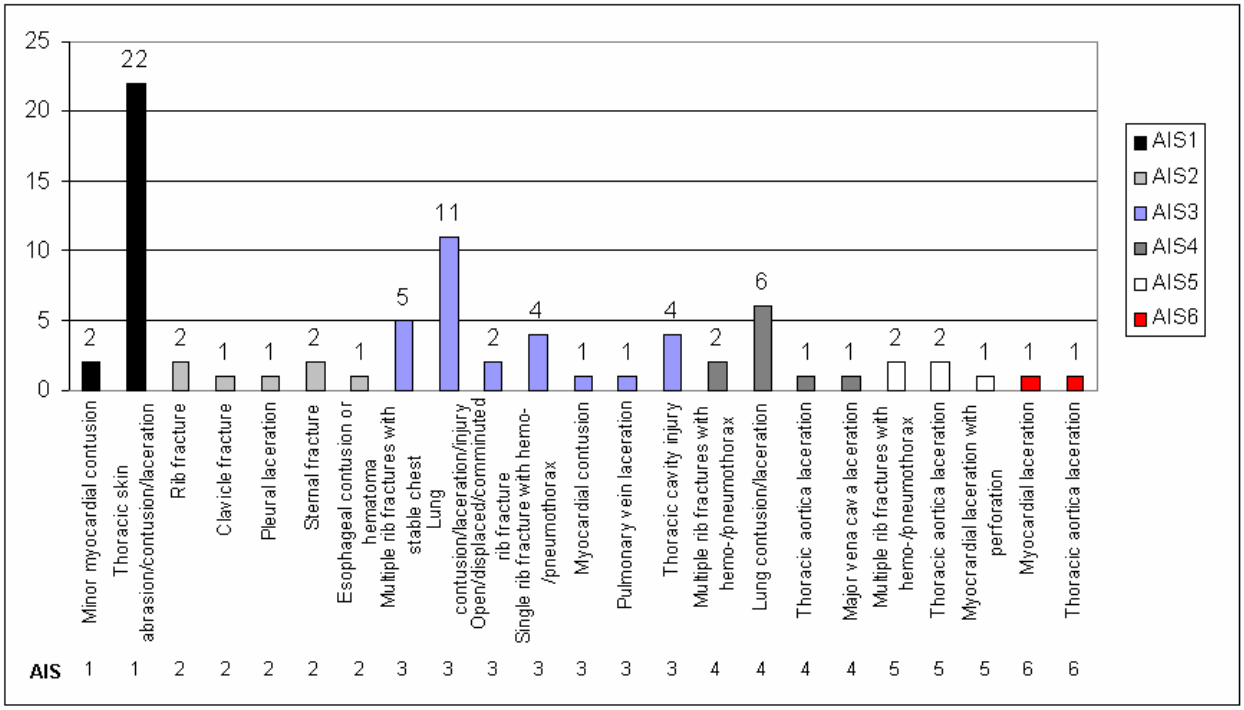

Figure 7 Injury to the abdomen, belted drivers in far side impacts in NASS for the years 2002 (n=27) and 2003 (n=32).

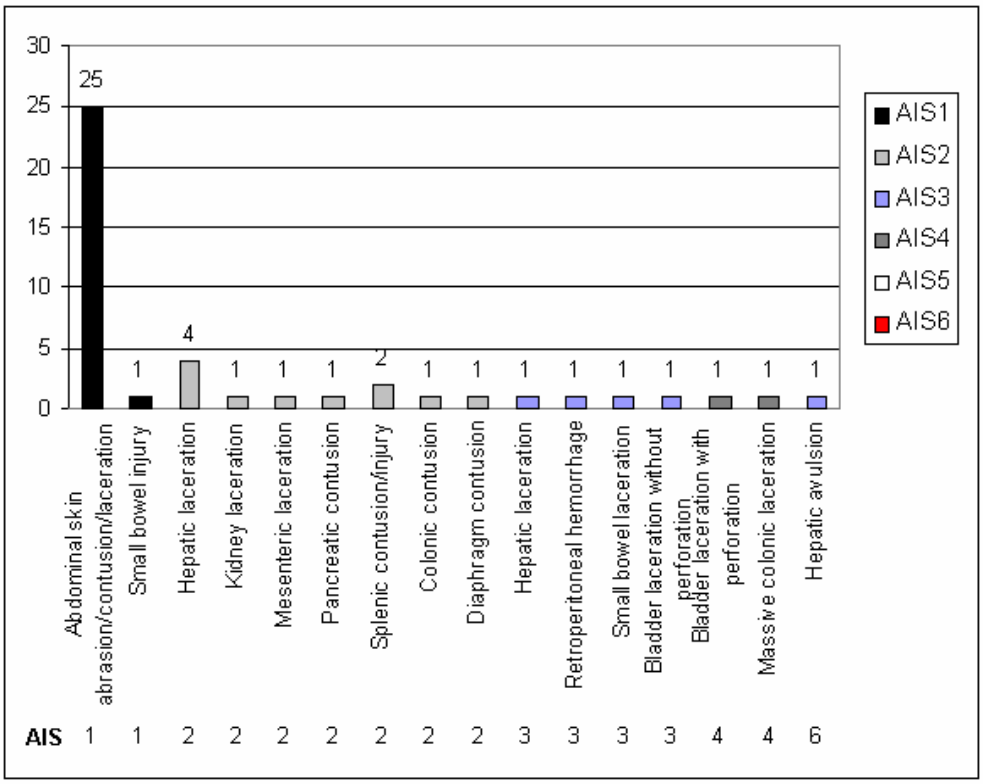

2.2 Summary

In summary, the priorities for the capabilities required for the test dummy and the associated injury risk functions for injury in far side impacts have to deal with the following for current restraint systems:

1. The highest priority injuries in far side crashes are to the head and face, spine, thorax, upper and lower limbs.
2. The impact direction (or crash PDOF) is between 30° and 90°.
3. The most common vehicle components involved are: the vehicle interior, restraint system, roof, seat, dash and steering.
4. The restraint system itself must not add to the serious injury.

3 AVAILABLE DUMMIES

Of utmost importance in a project based on the use of a dummy to predict impact injury, is that the dummy have high levels of biofidelity in its responses. The available test data indicates that the most biofidelic side impact dummy is the WorldSID, Hautmann et al. (2003) and Scherer et al. (2001). The biofidelity of the WorldSID, pictured in Figure 8, is compared with other side impact dummies in Table 4. The comparison inTable 4 is based on the methodology and test requirements from ISO 9790 (1999), Hautmann et al. (2003). The test results presented in Table 4 demonstrate why the injury risk functions still need to be matched to the specific dummy response as there are still significant short falls in the biofidelity ratings for some body regions of the WorldSID. Only limited information is available regarding the response of the WorldSID to 60° impacts. The need for the dummy to be used for far side impact testing to have an extensible spine is not fully met by the WorldSID. Of particular concern in this regard are the requirements of injury prediction in current vehicles and those fitted with more advanced safety systems, where the relative excursions and threat of injury will vary. For this reason comparative testing is being performed on the WorldSID for this project to specifically address far side issues.

Figure 8 The WorldSID prototype dummy.

Pintar et al. (2006) comments: “There are some limitations of this dummy for use in far side impact crashes, a mode that it was not originally designed for. Each of the ribs has an internally mounted IR-TRACC [Rouhana, et al., 1998] that measures deflection best when impacted directly lateral. Because of the interaction of the shoulder belt with the oblique portion of the lower rib cage for the outboard belt configuration, the abdomen deflections recorded in the present test series may be lower than actual oblique deflections at the location of belt interaction. Also, the design of the external portion of the shoulder region that interacts with the belt does not follow a human-like contour. For certain countermeasure belt designs where belt effectiveness depends on proper interaction with the shoulder, belt engagement may not be realistic in the current WorldSID design.”

Table 4 Comparison of the biofidelity of the SID, BioSID, ES-2 and prototype World SID side impact dummies using the ISO methodology, Hautmann et al. (2003).

		Test Biofidelity			
Requirement	**Test Description**	**SID**	**BioSID**	**ES-2**	**World SID**
Head Test 1	200mm Rigid Drop	0	10	5	10
Head Test 2	1200mm Rigid Drop	0	0	*	N.M.
Head Biofidelity		**0**	**6.7**	**5**	**10**
Neck Test 1	7.2 G Sled Impact	1.5	7	5.9	7
Neck Test 2	6.7 G Sled Impact	*	*	1.9	2.4
Neck Test 3	12.2 G Sled Impact	1.7	6	5.9	6.7
Neck Biofidelity		**1.6**	**6.7**	**4.4**	**5.2**
Shoulder Test 1	4.5 m/s Pendulum	2.9	5.7	2.9	6.1
Shoulder Test 2	7.2 G Sled Impact	0	7.5	2.5	10
Shoulder Test 3	8.9 m/s Padded WSU Sled	0	10	10	6.7
Shoulder Test 4		*	*	7.5	5
Shoulder Biofidelity		**1.2**	**7.3**	**5.3**	**6.7**
Thorax Test 1	4.3 m/s Pendulum	5	7.2	5	**7.8**
Thorax Test 2	6.7 m/s Pendulum	*	5	5	10
Thorax Test 3	1.0 m Rigid Drop	5	7.5	6.7	7.9
Thorax Test 4	2.0 m Padded Drop	5	7.7	*	N.M.
Thorax Test 5	6.8 m/s Rigid Heidelberg Sled	5	5	5.2	7.1
Thorax Test 6	8.9 m/s Padded WSU Sled	*	*	4.8	5
Thorax Biofidelity		**5**	**6.3**	**5.2**	**7.7**
Abdomen Test 1	1.0 m Rigid Drop	1.6	4.3	0	5.7
Abdomen Test 2	2.0 m Rigid Drop	3.5	3.2	1.1	6.8
Abdomen Test 3	6.8 m/s Rigid WSU Sled	*	*	5	8.3
Abdomen Test 4	8.9 m/s Rigid WSU Sled	*	*	1.3	5
Abdomen Test 5	8.9 m/s Padded WSU Sled	*	*	10	5
Abdomen Biofidelity		**2.5**	**3.8**	**2.6**	**6**
Pelvis Test 1	6.0 m/s Pendulum Impact	0	10	5	7.5
Pelvis Test 2	10 m/s Pendulum Impact	*	*	*	10
Pelvis Test 3	0.5 m Rigid Drop	2.5	5	8.3	5
Pelvis Test 4	1.0 m Rigid Drop	5	0	10	3.3
Pelvis Test 5	2.0 m Padded Drop	7.5	5	*	N.M.
Pelvis Test 6	3.0 m Padded Drop	*	*	*	N.M.
Pelvis Test 7	6.8 m/s Rigid Heidelberg Sled	0	2.2	0	7.8
Pelvis Test 8	8.9 m/s Rigid Heidelberg Sled	0	5	4.7	10
Pelvis Test 9	8.9 m/s Padded Heidelberg Sled	5	0	*	N.M.
Pelvis Test 10	6.8 m/s Rigid WSU Sled	*	*	4	6.9
Pelvis Test 11	8.9 m/s Rigid WSU Sled	*	*	1.6	5.9
Pelvis Test 12	8.9 m/s 15 psi Padded WSU Sled	*	*	10	5
Pelvis Test 13	8.9 m/s 23 psi Padded WSU Sled	*	*	7.8	5.6
Pelvis Biofidelity		**2.2**	**4**	**5.3**	**7.3**
Dummy Overall Biofidelity		**2.3**	**5.7**	**4.6**	**7.2**

The sign conventions used with the dummy are indicated in Figure 9 and the instrumentation fitted to the WorldSID in the tests at WMC, Pintar et al. (2006) for this project is summarised in Table 5. The injury risk functions developed in this report need to be supported by the available instrumentation fitted to the WorldSID. For use Instrumented upper and lower extremities are available for the WorldSID, Scherer et al. (2001), but were not used here.

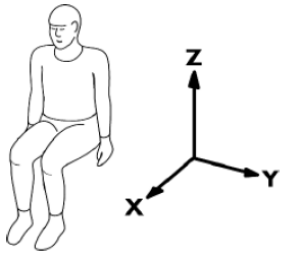

Figure 9 Sign convention used in the report

Table 5 WorldSID instrumentation used by WMC in testing for this project.

Channel Description	Axes	Filter	Units
Head CG Acceleration	X,Y,Z	CFC1000	G
Head Angular Acceleration	X,Z	CFC1000	RSS
Upper Neck Force	X,Y,Z	CFC1000	N
Upper Neck Moment	X,Y,Z	CFC600	Nm
Lower Neck Force	X,Y,Z	CFC1000	N
Lower Neck Moment	X,Y,Z	CFC600	Nm
T1 Acceleration	X,Y,Z	CFC1000	G
T4 Acceleration	X,Y,Z	CFC180	G
T12 Acceleration	X,Y,Z	CFC180	G
Pelvis Acceleration	X,Y,Z	CFC180	G
Shoulder Acceleration	X,Y,Z	CFC600	G
Thorax Rib 1 Acceleration	X,Y,Z	CFC1000	G
Thorax Rib 2 Acceleration	X,Y	CFC1000	G
Thorax Rib 3 Acceleration	X,Y,Z	CFC1000	G
Abdomen Rib 1 Acceleration	X,Y,Z	CFC1000	G
Abdomen Rib 2 Acceleration	X,Y,Z	CFC1000	G
Shoulder Displacement	Y	CFC600	mm
Thorax Rib 1 Displacement	X,Y,Z	CFC600	mm
Abdomen Rib 1 Displacement	X,Y	CFC600	mm
Shoulder Force	X,Y,Z	CFC600	N
Lumbar Force	X,Y,Z	CFC1000	N
Lumbar Moment	X.Y,Z	CFC1000	Nm
Pubic Force	Y	CFC1000	N

For the same reasons comparative testing will be performed as part of this project with THOR as the test subject for the 60° tests. THOR is an advanced frontal test dummy sponsored by the NHTSA, Haffner et al. (2001).

4 AVAILABLE INJURY RISK FUNCTIONS

The available injury risk functions for the individual body regions for injury causation and prediction and match with dummy capability, following the priority order:

4.1 Whole Body Lateral Loading of Restrained Volunteers

Zaborowski (1966) tested young male volunteers (n=52) to determine human tolerance to lateral impacts when wearing a restraint. The seatbelt used was a harness with two straps over the shoulders attached to a lap belt. The subjects were exposed to a total of 87 impacts at average accelerations from 4.5 to 11.6 g with no permanent physiological changes noted. The subject complaints (to 60%) increased above 8.8 g exposure. The experiments were halted for medical reasons after two subjects were subjected to the 11.6 g acceleration pulse. One of the subjects showed a marked cardiovascular response with rapid decrease in blood pressure and heart rate (brachicardia). Approximately 60 seconds post test the subject fainted in the seat. The author reported other similar results following lateral testing of volunteers.

4.2 Upper Extremities

Gabler (2004) found that the most common AIS3+ upper extremity injury were displaced and open fractures to the ulna (62%), to the radius (30%) and to the humerus (8%). Figure 3 gives the actual injuries to the upper extremities in far side crashes.

There are instrumented upper limbs available for the WorldSID, but these do not include instrumentation for the hand.

The most obvious injury criteria to use are long bone lateral fracture force and bending moment.

Lund (2003) suggested the following criteria for upper extremity injury based on work performed by Begeman (1999) and Pintar (1998) for the radius and ulna and by Kirkish (1996) for the humerus:

1. Lateral fracture force for the humerus (upper arm) is 214 Nm.
2. Bending moment for fracture of the ulna (forearm) is 90 Nm.

These values have been scaled by Mertz and Irwin (2003) for a range of occupants.

Sufficient data exists to turn these values into risk functions for fracture if required.
Duma et al. (1999) used a dynamic three point bending test with a 9.48 kg impactor, released from a drop height of 2.0 m to give an impact velocity of 4.42 m/s. This velocity was chosen to match radius and ulna strain rates as measured in cadaver tests with driver side air bags (Bass *et*

al., 1997). Three matched pairs of female forearms were tested with one forearm supinated and the other pronated to compare the differences. Within the three matched pair tests, the supinated position was significantly stronger ($p = .02$) than the pronated position with a 21% higher average peak moment of 92 ± 5 Nm versus 75 ± 7 Nm respectively.

Duma et al. (2003) developed injury risk functions for the 5th% female dummy. They presented equations for bending of the humerus and forearm and axial loading of the wrist and elbow.

$$\text{Forearm Moment} = \sqrt{(MX)^2 + (MY)^2}$$

$$\text{Humerus Moment} = \sqrt{(MX)^2 + (MY)^2}$$

$$\text{Wrist Load} = -FZ - (0.47) \cdot AZ$$

$$\text{Elbow Load} \quad \sqrt{(-FZ + (0.74) \cdot AZ)^2 + (FX + (0.74) \cdot AX)^2}$$

The risk functions predicted a 50% risk of injury at 128 Nm bending of the humerus, 58 Nm bending of the forearm, 1700 N axial loading of the wrist, and 1780 N axial loading of the elbow.

4.3 Head and Face

Injury priorities of body regions as a result of far-side impacts based on Gabler et al. (2005b) show the head and face as each individually having high priority. Head injuries were the most frequent injuries, caused the most Harm and were the most debilitating and life threatening injuries that occurred. The analysis also identified that head injuries of AIS 3 and greater severity caused the most Harm, and hence warranted priority in occupant protection considerations.

Gabler et al. (2005a) found that the leading source of injury to the head were contacts with the right interior (occupants in study were mainly drivers of left hand drive vehicles), roof, centre panel and right roof rail (shown in Figure 10).

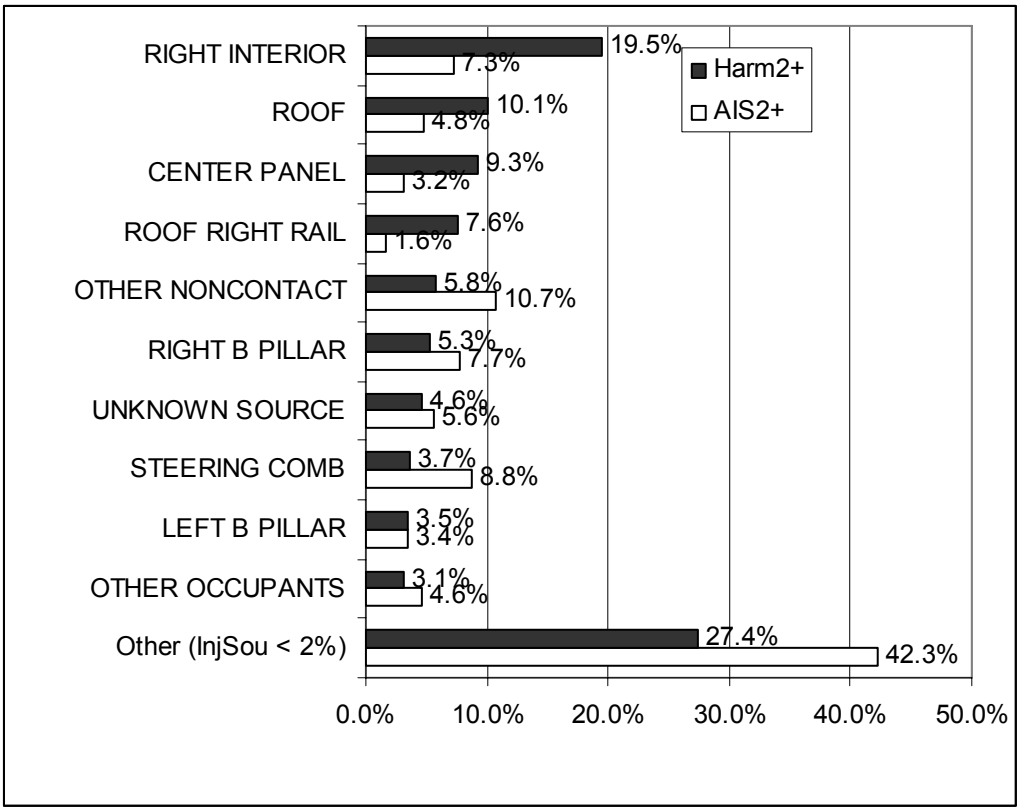

Figure 10 Source of AIS2+ head injury as a result of far-side impacts from Gabler et al. (2005a)

The direction of impact to the head and face in far-side collisions is not known at present. McLean et al. (1997) showed the location of fatal head injuries to vehicle occupants to be spread over the forehead, face, laterally and the crown, see Figure 11.

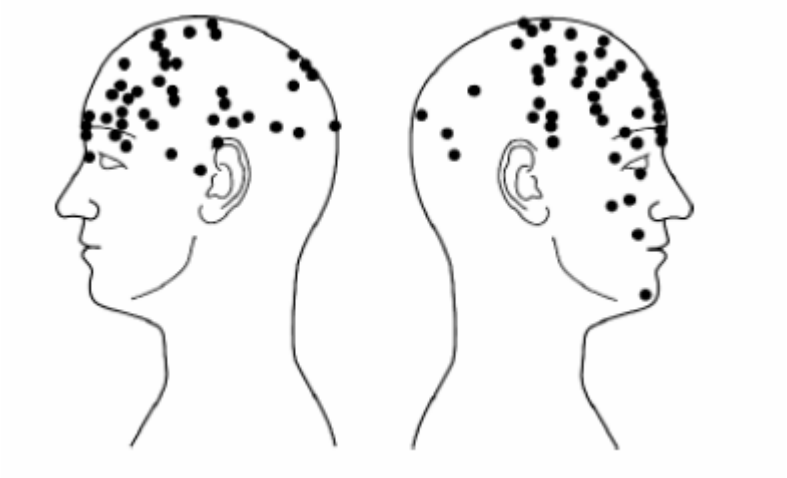

Figure 11 Location of fatal head injuries to car occupants, MacLean et al. (1997)

The real-world crash analysis suggests that, for the occupant on the non stuck side, the occupant will see lateral impacts to the head and also frontal and crown impacts. This suggests we want risk curves for the front and side or one set of curves that are sufficient to handle both conditions.

The WorldSID head is only calibrated for lateral impacts on a rigid surface. It is presumed the head is also valid for impacts to the forehead, as for HIII dummy.

The WorldSID head has both translational and rotational acceleration measurement capability.

The most commonly used indicator of head injury based on the acceleration of the head resulting from an impact, HIC (Head Injury Criterion) is defined as:

$$HIC = \max\left[\frac{1}{(t_2 - t_1)}\int_{t_1}^{t_2} a(t)dt\right]^{2.5}(t_2 - t_1)$$

where: $a(t)$ = resultant acceleration of the head's centre of gravity during the $t_2 - t_1$ time interval (G)
$t_2 - t_1$ = time interval during the acceleration pulse in which $a(t)$ attains a maximum value (ms)

HIC is based on the Wayne State University Concussion Tolerance Curve (Figure 12). This curve plots the effective translational acceleration of the head, which is an average anterior-posterior acceleration of the skull measured at the occipital bone, in impacts of the forehead with a rigid planar surface, against effective duration of the pulse (SAE 1980). The latter part of the curve with the asymptotic value of 42G is based on volunteer whole body data, which did not involve direct blows to the head. Patrick et al. (1965) recommended that this asymptotic value be raised to 80G. This revised level has been used as the basis of the U.S. Federal Motor Vehicle Safety Standards (FMVSS 208).

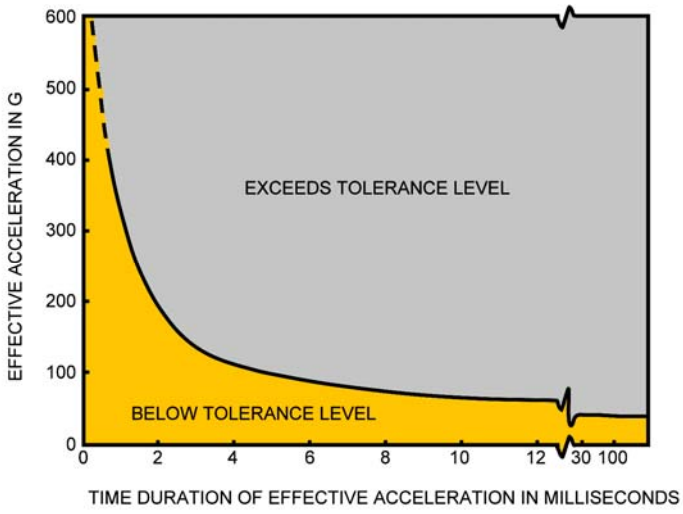

Figure 12 The Wayne State University Concussion Tolerance Curve, after SAE (1980).

Mertz et al. (2003) published a skull fracture risk curve with peak resultant acceleration of the head centre of gravity (CG) for the adult population, based on published cadaver head impact data. Using this, a 180G limit for the head acceleration as a result of direct impact for the 50th-percentile male Hybrid III dummy was proposed. This value is based on a 5% risk of skull fracture for the adult population, and represents a less than 5% risk for the mid-sized male.

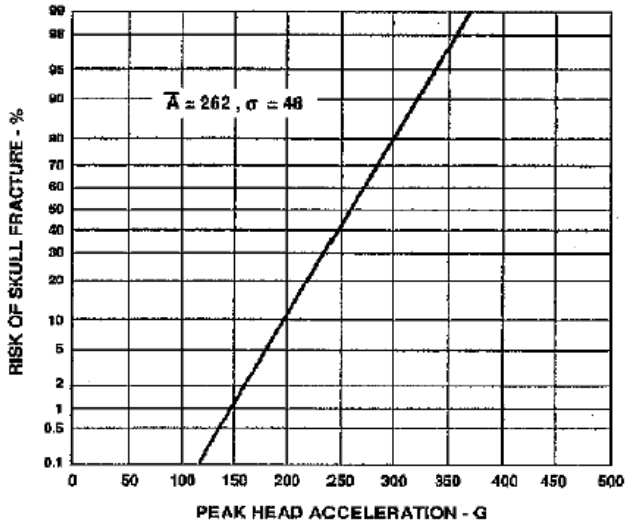

Figure 13 Skull fracture risk curve for the adult population based on peak head acceleration, from Mertz, Irwin, and Prasad (2003)

The recommended Injury Reference Values for HIC are the same as given in the Alliance (1999) recommendation to NHTSA for the OOP assessment of frontal airbags. For the average sized adult male, HIC of 700 corresponds approximately to a 5 percent risk of an AIS 4 or greater injury (Mertz et al., 1997). This value was scaled to give the Injury Reference Values for other sizes of occupants. The scaling method used takes into account size and brain tissue strength variation with age as described by Mertz et al. (1997). For all dummy sizes, the time interval of the search for the maximum HIC value was not to exceed 15 ms.

The curves proposed by NHTSA expanded from the Mertz/Prasad AIS 4+ brain injury curve go from AIS 1 (concussion) through to fatal head injury form an appropriate method for assessing the risk of head injury, see Figure 14 for the formulae and Figure 15 for a plot of the risk curves. These curves have reasonable matches with the other risk functions based on HIC available for comparison, such as for lateral head impact derived by Gibson et al. (2001) Figure 15 and the AIS 4+ brain injury risk curves derived by Mertz et al. (2003) for frontal impacts (Figure 16).

MAIS 1: $[1 + \exp((1.54 + 200/HIC) - 0.0065 \times HIC)]^{-1}$

MAIS 1: $[1 + \exp((2.49 + 200/HIC) - 0.00483 \times HIC)]^{-1}$

MAIS 1: $[1 + \exp((3.39 + 200/HIC) - 0.00372 \times HIC)]^{-1}$

MAIS 1: $[1 + \exp((4.9 + 200/HIC) - 0.00351 \times HIC)]^{-1}$

MAIS 1: $[1 + \exp((7.82 + 200/HIC) - 0.00429 \times HIC)]^{-1}$

Fatal: $[1 + \exp((12.24 + 200/HIC) - 0.00565 \times HIC)]^{-1}$

Figure 14 Formulae for the expanded Prasad/Mertz curves derived by NHTSA (1995).

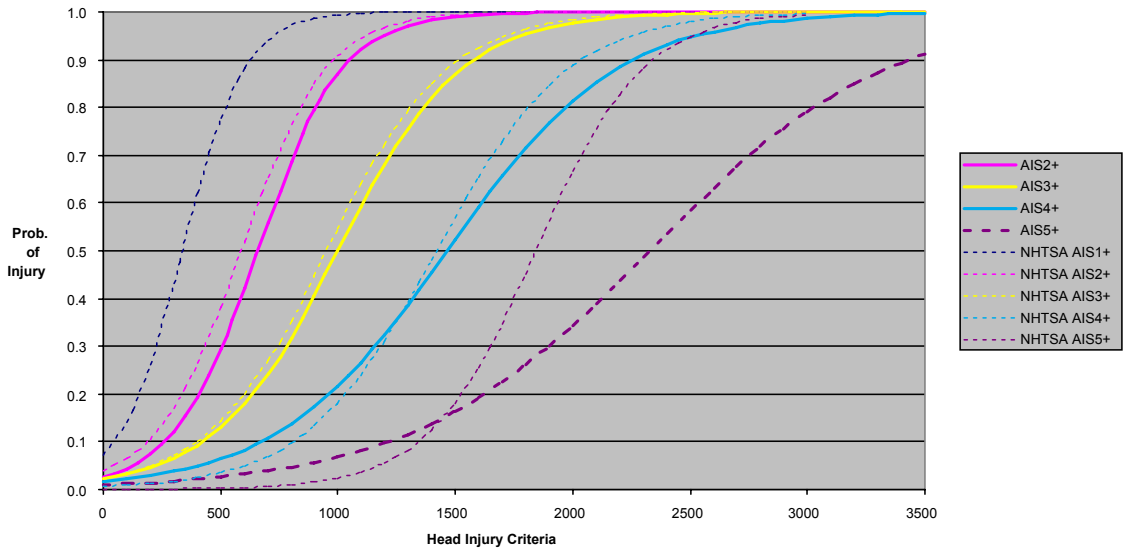

Figure 15 A comparison of the various risk of probability of head injury versus HIC curves the expanded Mertz/Prasad curves derived by NHTSA (1995) for frontal impacts to the head and AIS 2, 3, 4 and 5 curves derived by Gibson et al. (2001) for lateral impacts to the head.

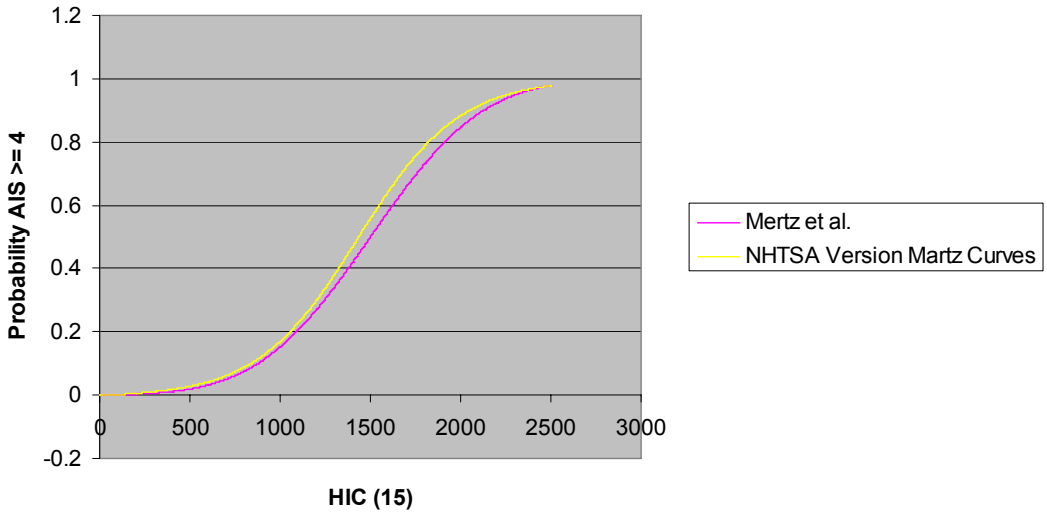

Figure 16 Comparison of the Mertz (2003) AIS4+ injury risk curve and AIS 4 NHTSA (1995) expanded curves for frontal impact.

At the low severity end, the AIS 1 curve for 15 ms impact durations Newman et al. (2000) reconstructed helmeted head impacts leading to MTBI in footballers. These researchers found that a 50% probability of concussion was found for a HIC of 240 and observed that the head was less sensitive to anterior posterior impacts than lateral.

The JARI Human Head Tolerance Curves, JHTC, were developed to overcome some of the deficiencies with the Wayne State curve. They generally supported the shape and values suggested in the WSTC. The frontal impact JHTC data show that the threshold for human skull fracture is slightly higher than that for cerebral concussion. The lateral head impact work at JARI was discussed in more detail by Kikuchi et al. (1982) and it was found that the tolerance for skull

fracture as a result of lateral impacts was lower than for sagittal and occipital impacts, but that the threshold for concussion was higher. Ono (1998) suggests, *". . . The concussion threshold against lateral impact . . . is located twice as high above the curve of sagittal [frontal] impact."*

Ommaya (1988) summarized the many experimental animal studies with which he had been involved, and extrapolated from the experimental data, proposing limits for allowable rotational acceleration for the human head. These limits are given in Table 6 He went further and suggested that a combined criteria was necessary for the prediction of head injury, and that such a criteria must link both rotational and translation effects.

Table 6 The allowable limits for rotational acceleration and velocity measured about the centre of gravity of the head, Ommaya (1988)

Rotational Velocity Change rad/s	Rotational Acceleration rad/s^2	AIS
>30	<1700	2
	<3000	3
	<3900	4
	<4500	5
<30	<4500	0 or 1
	<4500	5

Margulies and Thibault (1992) proposed human tolerance criterion for diffuse axonal injury specifically for lateral rotational loads to the head. This criterion was based on a combination of animal studies, physical models and analytical models. The animal data was scaled to human brain geometry and several different brain masses were used to derive threshold curves for the onset of moderate to severe diffuse axonal injury (DAI), see Figure 17.

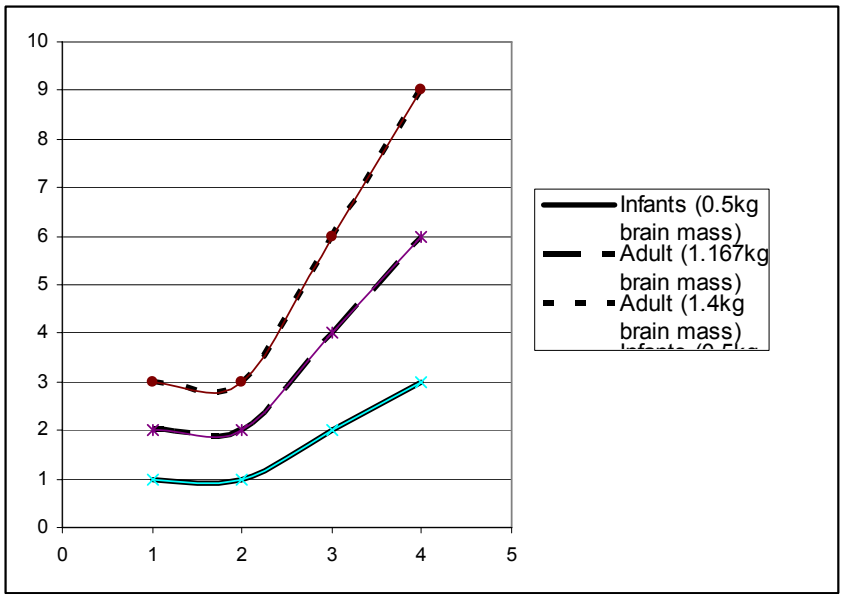

Figure 17 Moderate to severe diffuse axonal injury (DAI), thresholds for a range of human brain masses, for infant (500g brain mass, heavy solid line) and adult (1067g, solid line and 1400g, dashed line), Margulies and Thibault (1992)

Genarelli and co-workers studied the effects of pure angular acceleration, i.e., without direct impact to the head, on brain injuries. Their exhaustive research using subhuman primates and physical models led to the development of rotational acceleration thresholds for varying levels of brain injury including concussion, diffuse axonal injury (DAI), and subdural hematoma. More recently, Genneralli et al. (2003) synthesized these data and proposed angular acceleration thresholds for diffuse brain injuries as a linear function of varying severities (equation 3, R^2 = 0.99), described by the Abbreviated Injury Scale,

$$\dot{\omega} = 2.88 * AIS$$

where, $\dot{\omega}$ is the rotational acceleration (krad/sec2) and AIS represents the injury severity values in the length of unconsciousness section according to AIS 1998 version.

Rotational acceleration thresholds have been established from non contact experiments , Margulies and Thibault (1992). Other studies have examined angular acceleration magnitudes resulting from head contact. Meaney et al. (1994) used computer models of head contact to develop inertial loading conditions for diffuse brain injuries in minor to moderate collisions. A ΔV of 74 km/h was found to be needed to exceed the tolerance for concussion and "*yet higher velocities for mild to severe DAI*". These researchers' conclusions on the significance of head contact had support from real-world epidemiological studies, for example Morris et al.(1993). McLean found no cases with brain injury in the absence of evidence of head impact in an analysis of 414 fatal cases of road users in Australia.

4.4 Lower Extremities

Gabler (2004) found that the leading source of AIS3 lower extremity injury in far side cases were the result of contacts with the centre panel, the transmission lever followed by the right interior of the vehicle. The most common injury was found to be fractures of the long bones, the femor, tibia and fibula. Injury to the knee and ankle joints also needs to be considered.

There are existing IAFs for the lower extremities but these mainly relate to frontal impacts, Mertz (2003). The use of the injury criteria for long bone bending for pedestrian impacts based on Ivarsson et al. (2004) and others is a good approach. This is supported by the IIHS side impact requirements, IIHS (2004). This may require some further work to develop IAFs.

The IIHS (2004) report on side impact test program rating specifies a degree of acceptability for distal femur A-P and L-M moment (3 msec clip) of an M_{femur} of 255 – 305 Nm.

Konosu et al. (2005) of the Japan Automobile Research Institute (JARI) reviewed recent lower leg injury tolerance, which are summarized in Table 7 below.

Table 7 Recent lower leg injury tolerance values for pedestrian leg impacts selected by Konosu et al. (2005).

Body regions		50% injury risk level for 50 percentile American male (tentative)	References
Leg		BM (312 - 350 Nm)	BM (312 Nm): Kerrigan et al., 2004 BM (350 Nm): INF GR/PS/82
Knee	MCL	EL (18 - 20 mm)**	BA (18 deg).: Ivarsson et al., 2004 BA (20 deg).: INF GR/PS/82
	ACL	EL (10 mm)***	SD (10 mm): IHRA/PS/309
	PCL	EL (10 mm)***	SD (10 mm): IHRA/PS/309
Thigh		BM (372-447 Nm)	BM (372 - 447 Nm): Kerrigan et al., 2004 BM (390 - 395 Nm): Kennedy et al., 2004

* BM: Bending moment, EL: Elongation, BA: Bending angle, SD: Shearing displacement.
** Estimated from BA (18-20 deg.), *** Estimated from SD (10 mm)

Kerrigan et al. (2004) found the risk function for femur fractures (see Figure 18) to be:

p(femur fracture) = 1 – EXP [-EXP(6.24242 ln(M_{max}) – 38.45762)] .

Kennedy et al. (2004) did 45 experiments on the femur of PMHS using a dynamic three-point drop test. They found no significant difference between the lateral-medial bending experiments and the posterior-anterior bending experiments. These investigators determined

p(femur fracture) = 1 – EXP {-EXP[7.1613 ln (M_{max}) – 42.987]}

as the risk of femur fracture for the 50th% male.

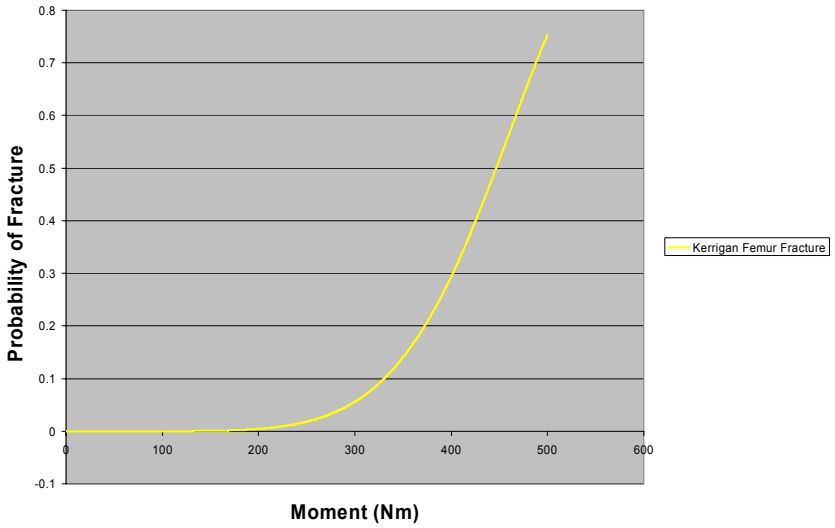

Figure 18 Femur fracture risk function from Kerrigan et al. (2004).

Kerrigan et al. (2004) also found a risk function for tibia fractures:

$$\textbf{p(tibia fracture)} = 1 - EXP[-EXP(5.69112 \ln(M_{max}) - 33.05211)]$$

Mertz et al. (2003) also propose a tibia shaft fracture risk curve for the adult male population based on maximum bending moment:

$$\textbf{Probability density function} = EXP[-((M - 317)2)/(15{,}488)]/(220.5833)$$

$$\textbf{p(tibia fracture)} = \int_0^M \textbf{(probability density function) dM}$$

These two functions give very similar results when plotted, see Figure 19.

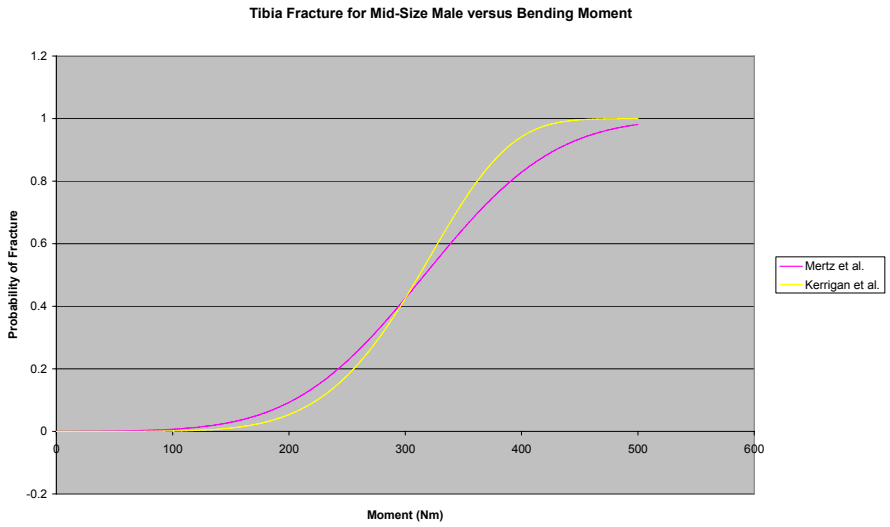

Figure 19. Comparison of the tibia fracture risk functions proposed by Mertz et al. (2003) and Kerrigan et al. (2004)

4.5 Spine

The most representative testing for real crashes of the strength of regions of the spine is of complete spines. The discussion here will only be on the literature on the failure properties of multiple vertebral body spinal segments of the thoracolumbar spine, which is the most limited of the three main areas of spinal failure property research. However, there are a few studies that provide valuable insight into the failure properties and failure mechanisms of multiple thoracolumbar vertebral body spinal segments (Yoganandan, 1988; Myklebust, 1989; Duma, 2006). The testing type, failure properties, and failure modes of these studies have been summarized (Table 8).

There have been no studies that have investigated the failure properties of multiple thoracolumbar vertebral body spinal segments in lateral bending. However, Demetropoulos (1988) conducted sub-failure stiffness testing on 10 multiple lumbar vertebral body spinal segments, T12-L5, in compression, tension, flexion, extension, lateral bending, anterior shear, posterior shear, and lateral shear. The average maximum sub failure moment in lateral bending

was reported to be 113 Nm. The average maximum sub failure load in anterior shear, posterior shear, and lateral shear was reported to be 830 N, 1760 N, and 150 N respectively.

The Chandler and Gaudy (1983) developed a lumbar spine injury criteria for the HII dummy based on injuries occurring during ejections from military aircraft of a 5% risk of injury for a compression load of 6.7 kN. This is used by the Federal Aviation Authority (FAA) for testing aircraft seats, FAA (1996).

Table 8. Failure properties of multiple vertebral body spinal segments

Reference	Spinal Level	Experiment	Loading Rate	Average Failure Load (N)	Average Failure Moment (N-m)	Failure Mode
Yoganandan (1988)	T3-L5 (9) T2-L5 (4) T4-L5 (1) C2-L5 (2) T6-L5 (2)	compression-flexion	2.5 mm/s	2344 1192 444 679 5418	177 99 289 84 284	Spinal column fracture due to wedging (T10-L2)
	T2-L3 T3-L2 T8-L3	Three-point Bending (flexion)	2.5 mm/s	1681 2170 1432	201 326 129	Center of spine at point of maximum flexural moment
	T12-L5 T4-L4 T10-L2	Four-point Bending (flexion)	2.5 mm/s	4893 1712 1544	245 86 77	Center of spine at point of pure flexural moment and no shear
Myklebust (1989)	T2-T9 T10-L1 (n=14)	compression (neck flexed)	ranged from 10-1200 mm/s	1223 2680	N/R	Wedge fractures from T9-L1
	intact cadaver (n=4)	Compressive load applied to T1	10 mm/s	1788	N/R	wedge /compression fractures at thoracolumbar junction
Duma (2006)	T12-L5 (n=2)	Axial compression (anatomically oriented in seated position)	1000 mm/s	5460	201	wedge /compression fractures of T12
FAA (1996)	Compressive lumbar load limit during restraint system testing POD in line with spinal column		dynamic	6672	-	N/A

4.6 Thorax

Gabler et al. (2005a) found that the leading source of AIS2+ chest injury were contacts with the seat back, the belt webbing or buckle, the right interior (occupants in study were mainly drivers of left hand drive vehicles) and other occupants. The most serious chest injury occurred as a result of impacts resulting in a PDOF of 60°.

Chest IARVs for acceleration of the chest spine (at the T4 vertebra) were proposed by the General Motors Corporation for the 50th-percentile male Hybrid III dummy, Mertz (1984). A

60G limit was imposed based on human volunteer rocket tests (Stapp, 1970) and stunt diver tests (Mertz & Gadd, 1971). A resultant T4 acceleration less than 60G (3 ms criterion) represents a less than 5% risk of significant thoracic organ injury (AIS ≥ 3) due to gross chest acceleration. Note that significant injury may still be produced by other means such as chest compression or sternal loading.

Kuppa et al. (2004) suggested an injury assessment curve based on lateral chest deformation based on 34 side impact tests using PMHS, see Figure 20.

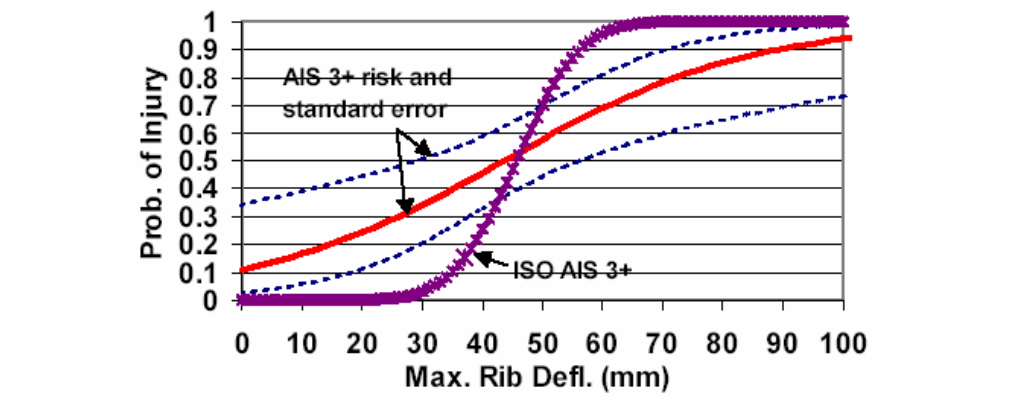

Figure 20. Comparison of the AIS 3+ probability of thoracic injury suggested by Kuppa et al. (2004) for with the ISO (2004) risk curve for the EuroSID 1 for rib deflection.

Viano et al. (1995) suggested that it was necessary to use a viscous criterion as well. A V*C value of 1.0 m/s, represents approximately a 5 percent risk of AIS 4+ thoracic injury.

The IIHS (2004) guidelines suggested that a peak deflection 50 mm and a peak V*C of 1.01-1.2 was acceptable.

The ISO (2005) injury risk curves for the chest responses of the WorldSID dummy were developed based on selected PMHS test data, see Figure 20 and Figure 21.

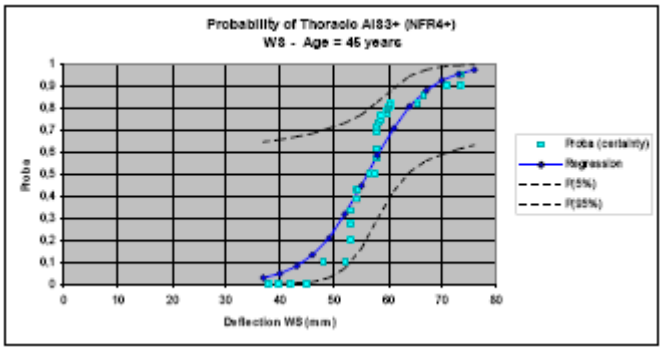

(a)

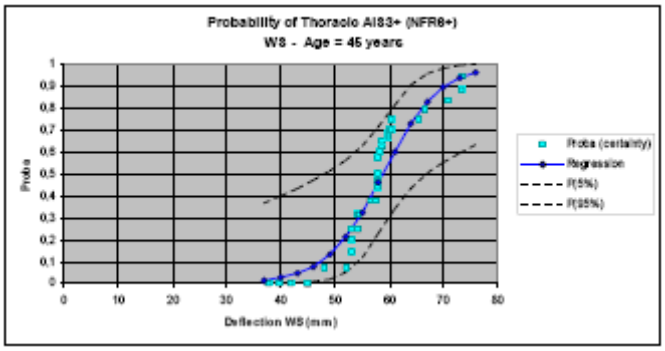

(b)

Figure 21 Injury risk functions for lateral chest deflection of the WorldSID dummy, from ISO (2005).

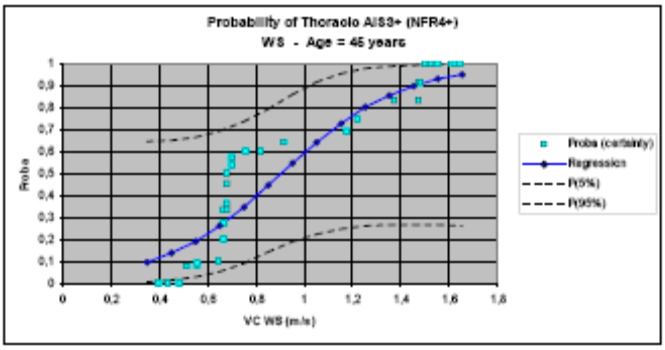

(a)

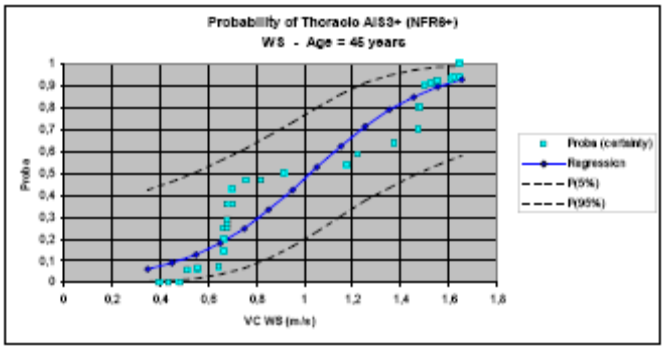

(b)

Figure 22 Injury risk functions for lateral chest V*C of the WorldSID dummy, from ISO (2005).

4.7 Abdomen

Gabler et al. (2005a) found that the leading source of AIS2+ abdominal injury were the result of contacts with the safety belt webbing or buckle (86%), followed by the right interior (7%). For the AIS 3+ injuries the seat belt and buckle were still the most common source of injury (37%), but contacts with the other occupant (10%) transmission lever (9%) and right interior (8%) were significant sources. The most serious abdominal injury occurred as a result of impacts with a PDOF of 90°.

Kuppa (2004) suggested an abdominal injury assessment curve based on total internal abdominal force for the ES 2re, see Figure 23.

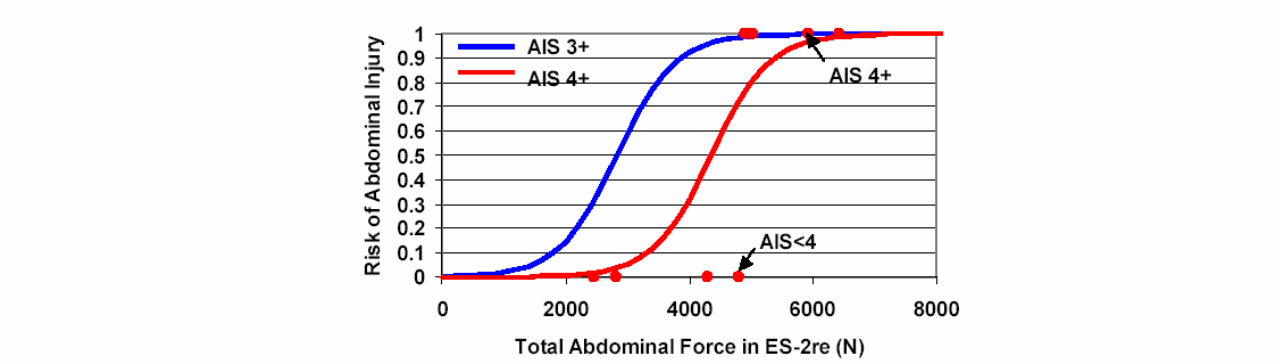

Figure 23 Injury assessment curve based on total internal abdominal force for the ES 2re, Kuppa (2004).

Mertz et al. (2003) suggested a limit on internal abdominal load of 2,500 Newton.

Rouhana et al. (1985) based on testing with rabbits, found abdominal trauma correlates with V*C.

The IIHS (2004) report sets side impact testing guidelines and rates a V*C of 1.01 – 1.2 as acceptable for the abdomen in lateral crashes.

In ISO (2005) injury risk curves for abdominal responses of the WorldSID dummy were developed based on selected PMHS test data, see Figure 24. These functions were based on lower spine acceleration, abdominal deflection and V*C for the dummy.

(a)

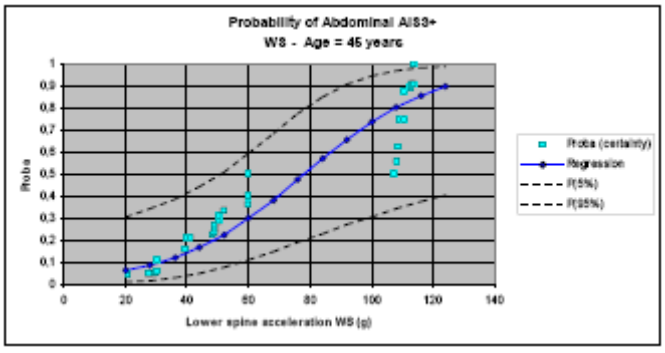

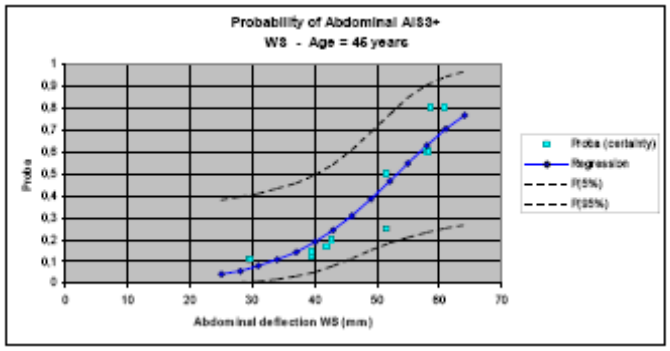

(b)

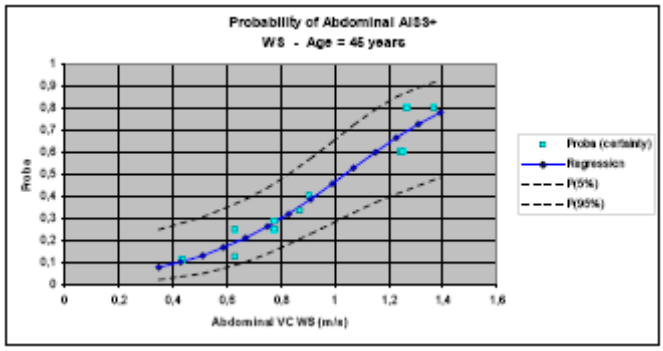

(c)

Figure 24 Injury risk functions for lateral abdominal responses of the WorldSID dummy, from ISO (2005).

4.8 Neck

The conundrum for the choosing a neck injury criterion is that the only existing combined load neck injury risk function is based on N_{ij}. It was developed and validated based on axial loading, flexion and extension of the neck in frontal impacts, in the mid-sagittal plane. Most likely loading is going to be tension compression with lateral bending and axial twisting. We have no neck injury risk functions for the lateral direction. If we follow the IIHS (2004) approach of using the values developed for the frontal direction, then we need to develop an interpretation that gives a reason for going forward.

An alternative approach used by WTG and IIHS, Lund (2003) for side impact neck injuries is to use a risk function for axial force and monitor the magnitude of the x axis moment (lateral bending) and the z axis moment or neck twist.

Mertz et al. (2003) propose a risk of AIS ≥ 3 neck injury based on normalized tension, $F_{tension}$ / $F_{critical}$, where $F_{critical}$ = 3,290 Newtons. This is based on no muscle tone for the neck. The resulting risk curve for neck tensile loading is plotted in Figure 25.

$$\textbf{Probability density function} = \textbf{EXP}\left[-\left(\left(F_{tension} / F_{critical} - 1.250\right)2\right)/(0.034848)\right]/(0.330875)$$

$$p(\text{AIS} \geq 3) = \int_{0}^{F_{normalized}} (\text{probability density function})\, dF$$

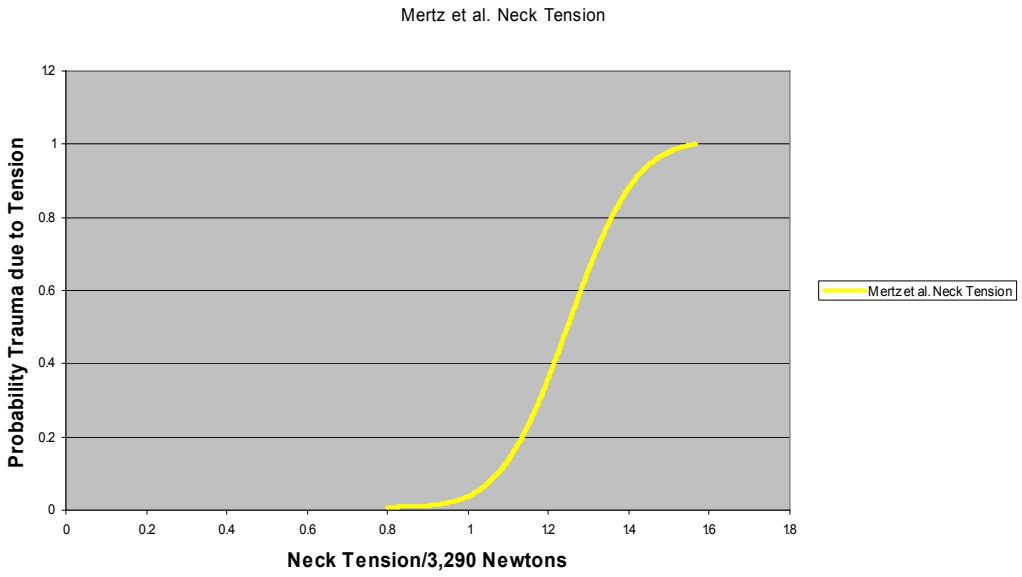

Figure 25. Injury risk curve for neck tensile loading Mertz et al. (2003)

4.9 Shoulder

Bolte et al. (2000) used pneumatic impacting ram was employed in carrying out twenty two lateral impacts to eleven unembalmed human cadavers at the level of the glenohumeral joint. The objective of this study was to determine response characteristics and injury of the shoulder due to lateral impacts, at a ram velocity of 3.5 to 7.0 m/s. The most common result was a loosened acromio-clavicular joint and a distal fracture of the clavicle occurred in 9 cases, approximately 1-2 cm from the acromio-clavicular joint. A maximum deflection of 47 mm between the impacted acromion and the sternum lead to approximately half of the impacts resulting in an AIS level 2 injury. The peak force varied with the velocity from 1550 to 4130 N.

Mertz et al. (2003) suggest several shoulder injury criteria:

- Limiting the peak lateral shoulder force to 4000 N or less; and,
- Limiting the peak lateral deflection to 75 mm or less.

4.10 Pelvis

Kuppa (2004) suggests a pelvic injury assessment curve based on pubic symphysis force of the ES-2re dummy, see Figure 26.

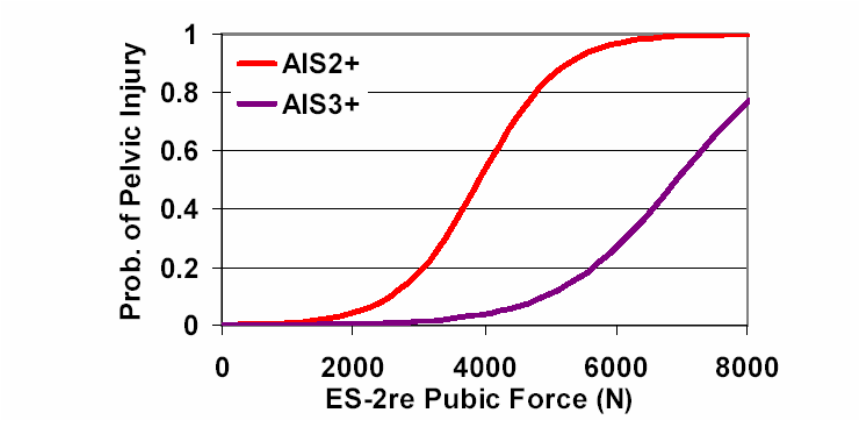

Figure 26. Pelvic injury assessment curve based on pubic symphysis force of the ES-2re dummy, Kuppa (2004)

The IIHS (2004) report sets side impact testing guidelines and rates a Fpelvis of 4100 – 4800 N to be acceptable. IIHS also uses combined acetabulum and ilium forces of less than 4.8 kN for either or 6.1 kN combined and pelvic acceleration

In ISO (2005) pelvic fracture risk curves for the WorldSID dummy were developed based on selected PMHS test data, see Figure 27. These functions were based on pubic force and pelvic acceleration.

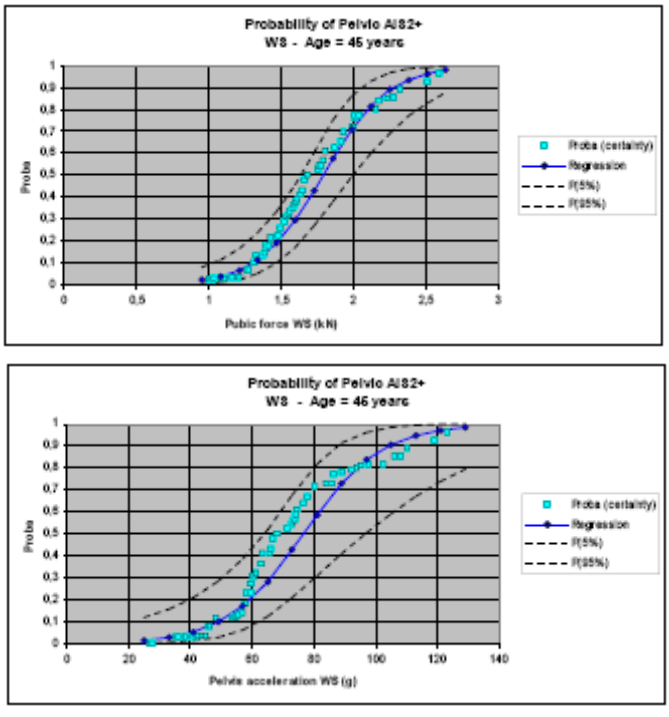

Figure 27 Pelvic fracture risk curves for the WorldSID dummy, ISO (2005)

Mertz et al. (2003) suggested limiting the iliac crest, pubic, and sacrum loading to:

- Peak iliac crest load to 6000 Newton.
- Peak pubic load to 6000 Newton.

- Peak sacrum load to 6000 Newton.

Kuppa (2004) says 6,000 Newtons is about a 25% probability of an AIS ≥ 3 injury in the abdominal region.

The ISO says 6,000 Newtons is about a 52% probability of a pelvic fracture.

5 PROPOSED INJURY RISK CURVES

5.1 Risk Curves for the Head

Ono (1998) discusses the fracture threshold for front and side and the concussion threshold for front and side.

> "However, the temporal fracture threshold shows a value ... approximately 50 percent of the fracture threshold on frontal and occipital impact ....
>
> ... the concussion threshold curve of lateral impact. The entire curve is located twice as high above the curve of sagittal impact."

In other words, the Ono study suggests using the frontal curve for the side would give more fractures and fewer concussions.

In animal tests, Dixon (1998) studied the presence or absence of a summed neurological score after 50 minutes and discussed his findings.

> "... central and lateral impacts .. illustrates similar functions in regard to the acute neurological responses."

Using HIC as the dependent variable, Gibson (2001) analyzed 55 (after dropping 3 outliers) lateral impacts to PMHS heads. The analysis suggests that the lateral risk curves are similar to frontal risk curves for the head.

In writing the support document for a Notice of Proposed Rulemaking for Federal Motor Vehicle Safety Standard, Kuppa (2004) equated the lateral HIC criterion to the frontal HIC criterion.

The real-world crash analysis suggests that, for the occupant on the non stuck side, the occupant will see lateral impacts to the head and also frontal and crown impacts. This suggests we want risk curves for the front and side or one set of curves that are sufficient—given the present stage of biomechanical research—to handle both conditions

The injury risk curve proposed for use with the WorldSID is the Mertz et al. curve published in 2003. The curve assumes a normal distribution with mean and standard deviation shown in Table 9.

Table 9. Probability of Brain Injury

Body Region	Independent Variable	Mean Value	Standard Deviation
Head	HIC (15)	1,434	430

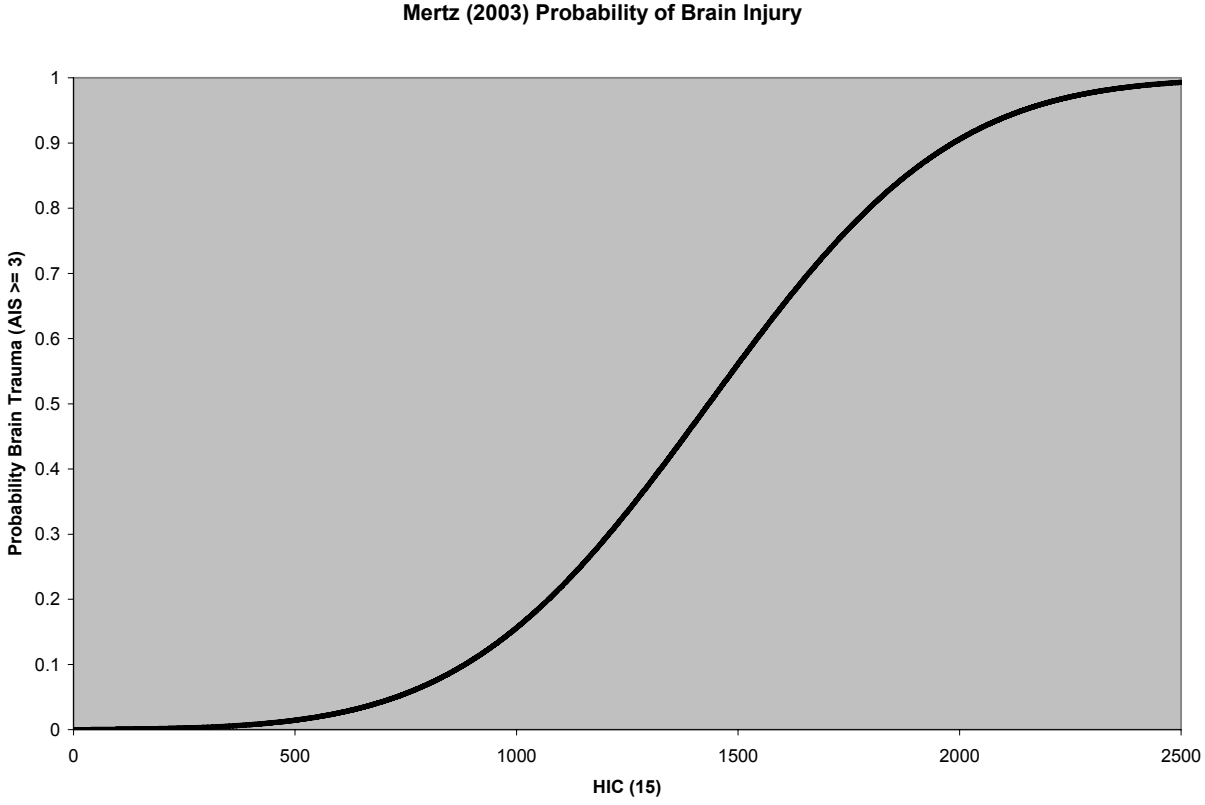

5.2 Injury Risk for the Neck

AIS ≥ 3 neck injury risk is based on normalized tension, $F_{tension} / F_{critical}$, where $F_{critical}$ = 3,290 Newtons. The resulting risk curve for neck tensile loading is

$$\textbf{Probability density function} = \textbf{EXP}\left[-((F_{tension} / F_{critical} - 1.250)\,2)/(0.034848)\right]/(0.330875)$$

$$p(\text{AIS} \geq 3) = \int_{0}^{F_{normalized}} (\text{probability density function})\, dF$$

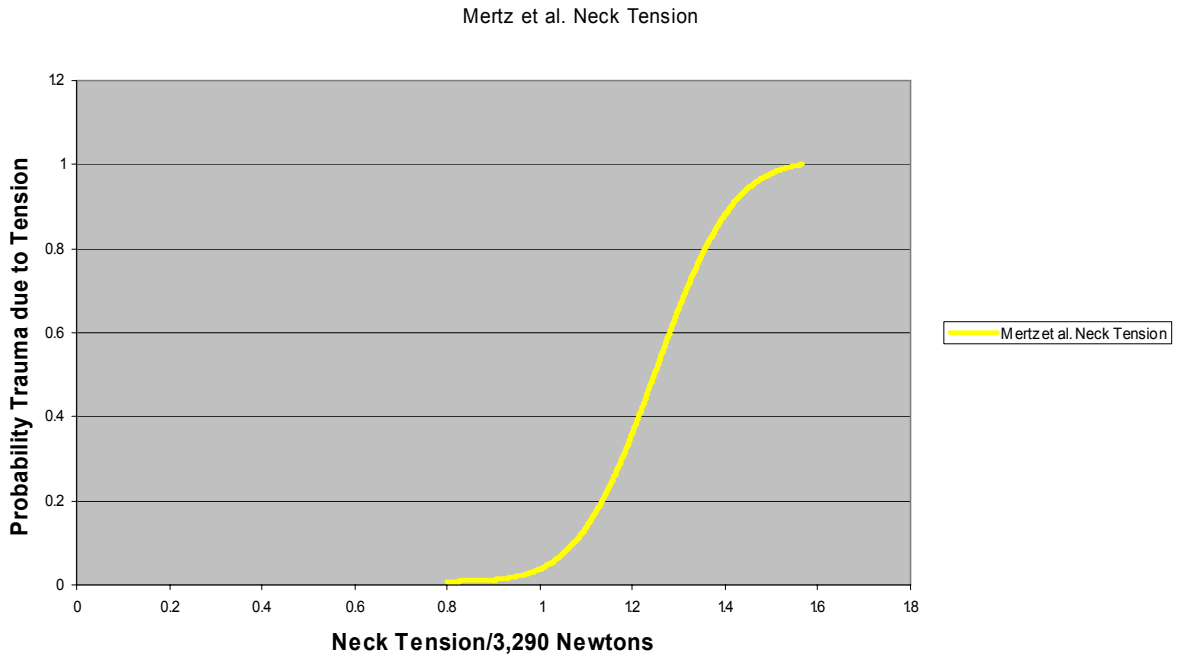

Figure 28. Injury risk curve for neck tensile loading Mertz et al. (2003)

An allowable upper cutoff point on neck shear is specified.

Body Region	Independent Variable	Mean Limit
Neck	Shear (N)	3100

5.3 Injury Risk Curve for the Chest

The ISO suggested an injury assessment curve based on lateral chest deformation. The ISO risk curve has a stepper sigmoidal shape than a chest deflection curve proposed by Kuppa. The ISO also put forward a VC risk curve.

5.4 Risk Curve for the Chest

Body Region	Independent Variable	Mean Value	Standard Deviation
Chest	Maximum Chest Deflection (mm)	56.1	9.1

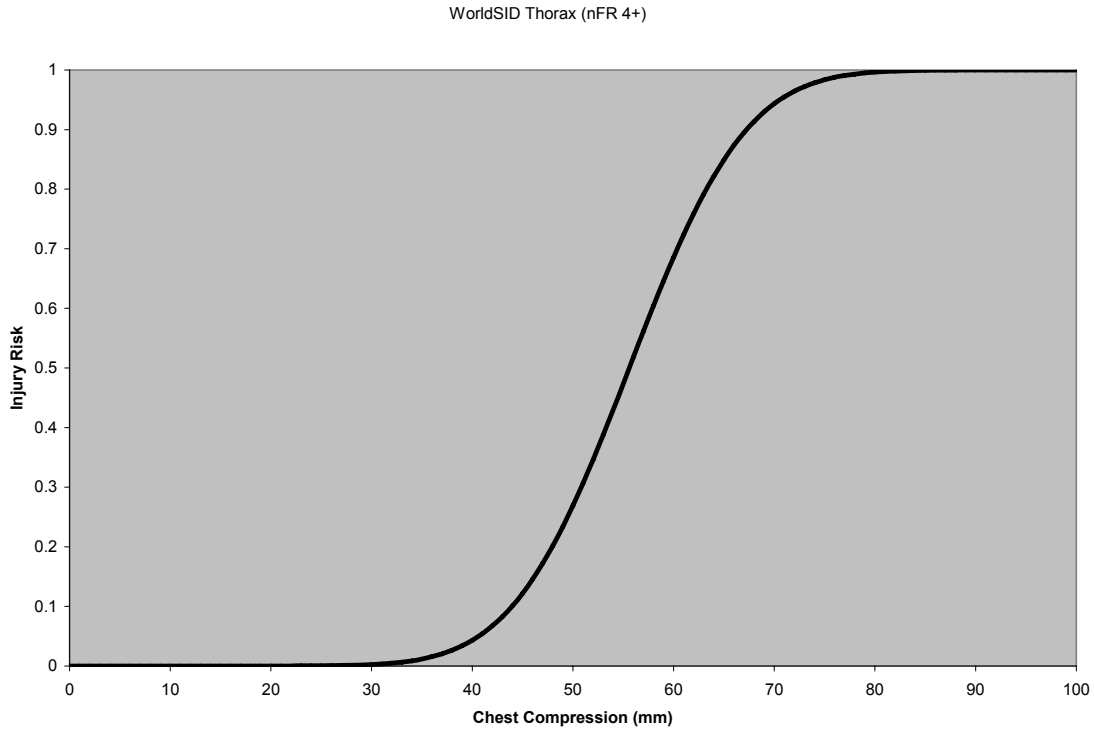

Figure 29 Risk curve for the chest deflection

Body Region	Independent Variable	Mean Value	Standard Deviation
Chest	V*C (m/s)	0.9	0.41

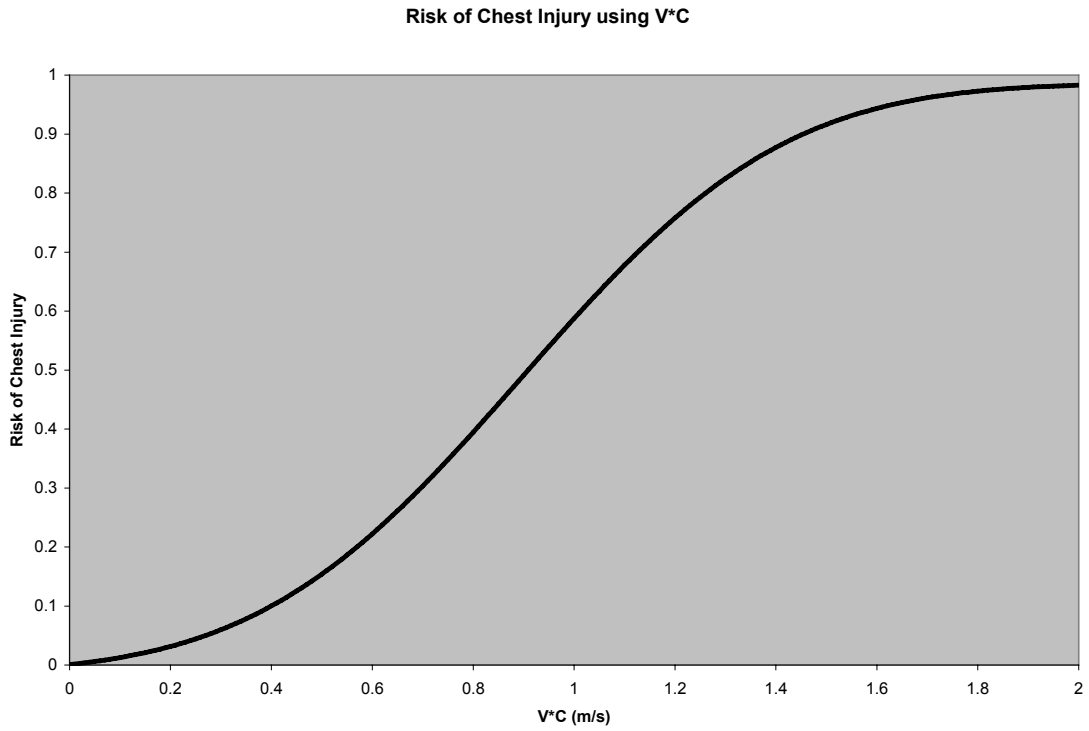

Figure 30 Risk curve for the V * C

5.5 Injury Risk Curve for the Abdomen

Kuppa suggested an injury assessment curve based on internal abdominal force. The ISO suggested an injury assessment curve based on internal abdominal force. Mertz et al. suggested a limit on internal abdominal force.

Based on testing with rabbits, Rouhana et al. found abdominal trauma correlates with V*C.

Body Region	Independent Variable	Mean Value	Standard Deviation
Abdomen	Maximum Abdomen Compression (mm)	53.2	15.1

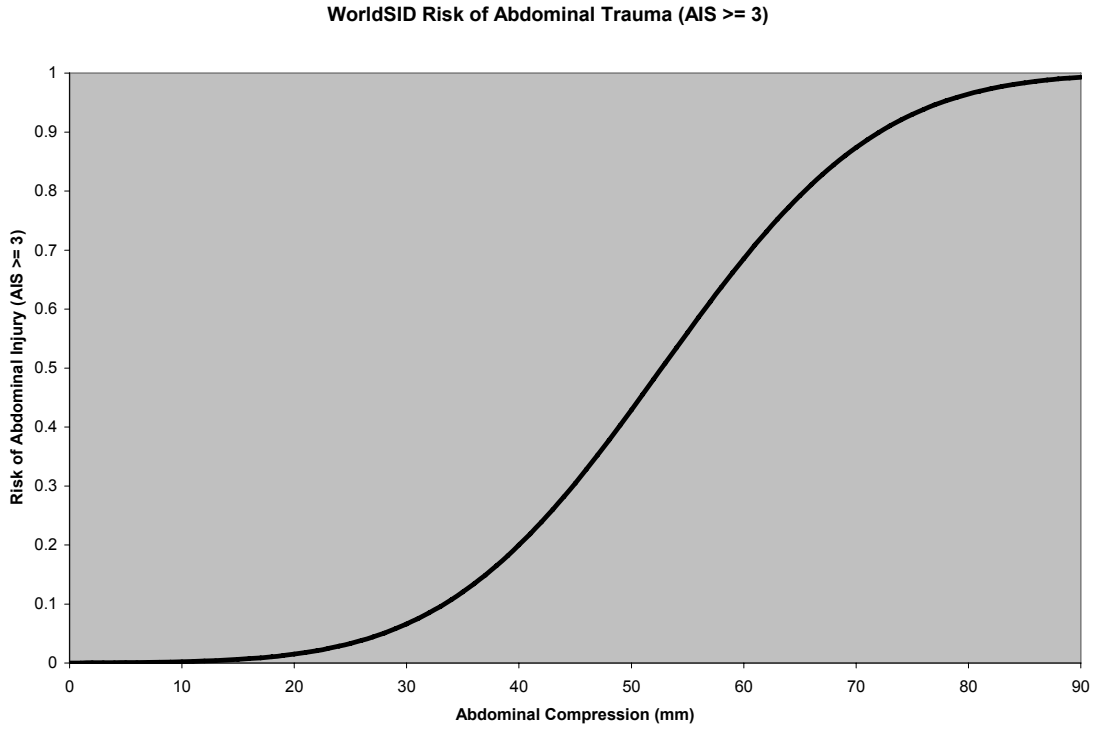

Figure 31 Risk curve for the abdomen deflection

Body Region	Independent Variable	Mean Value	Standard Deviation
Abdomen	V*C (m/s)	1.03	0.46

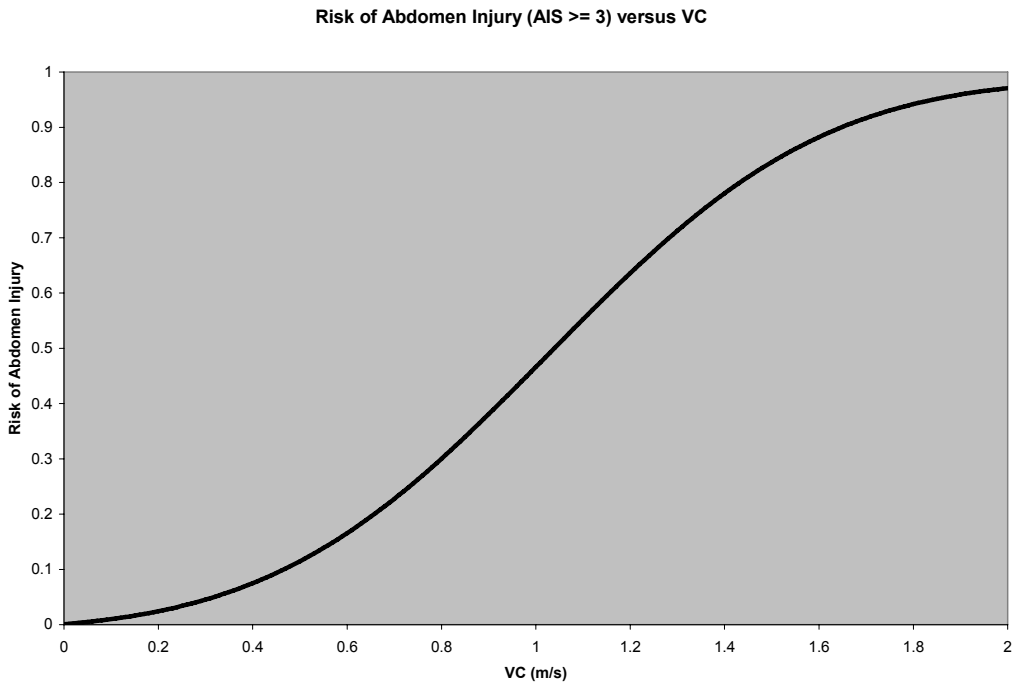

Figure 32 Risk Curve for the abdomen V * C

5.6 Injury Risk Curve for the Pelvis

Kuppa suggested an injury assessment curve based on pubic symphysis force. The ISO suggested an injury assessment curve based on pelvic force. Mertz et al. suggested a limit on iliac crest, pubic, and sacrum load.

The WorldSID pelvis is very different from that of other dummies. "The pelvis consists of a conical shaped polyurethane pelvic bone that mimics the human pelvic bone. The major landmarks of the WorldSID dummy are close to the anatomical data. A vinyl skin surrounds the pelvic bone and this skin is filled with an elastomer. The hip joint of the WorldSID dummy consists of a ball and socket joint, this is a different configuration from the existing side impact dummies which all have hyme joint construction." In contrast, the EuroSID2, SID, and BioSID all have a fairly rigid metal pelvis surrounded by simulated flesh. This may lead to a different response than what researchers are currently expecting of a dummy pelvic response.

As a consequence of this design direction, the risk curves for pelvic trauma are two in number. The first risk curve, for external pelvic loading, is based on the independent variable acceleration. The second risk, for loading going through the pubic symphysis, is based on the independent variable pubic force.

Body Region	Independent Variable	Mean Value	Standard Deviation
Overall Pelvis	Acceleration (G)	76.6	21.2

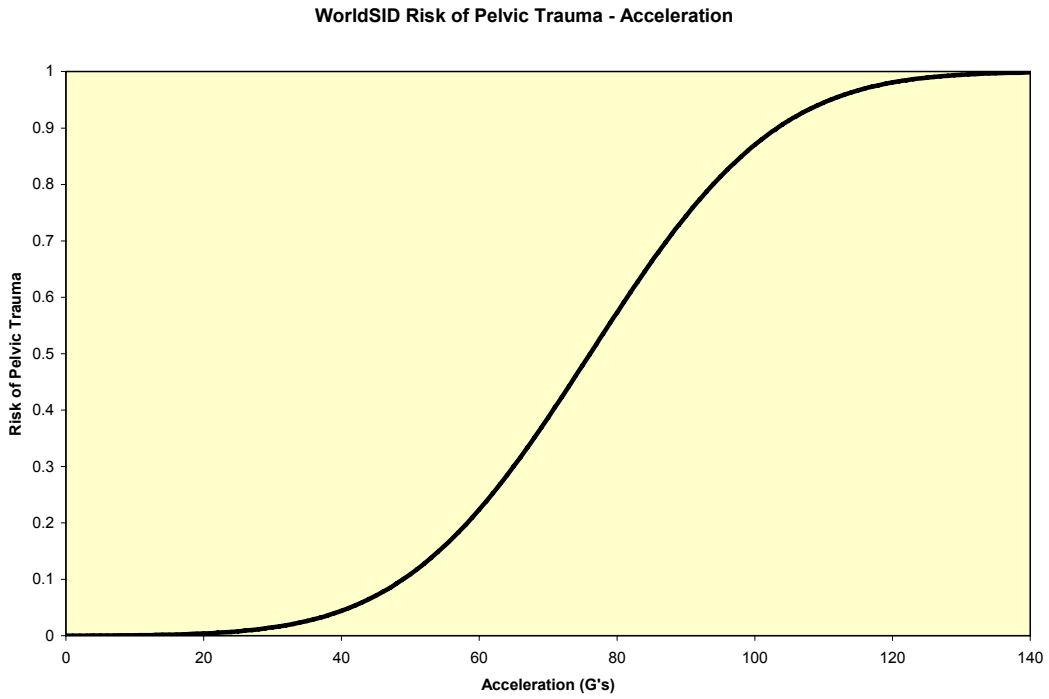

Figure 33 Risk curve for the pelvis acceleration

Body Region	Independent Variable	Mean Value	Standard Deviation
Pelvis Symphysis	Pubic Force (N)	1,800	400

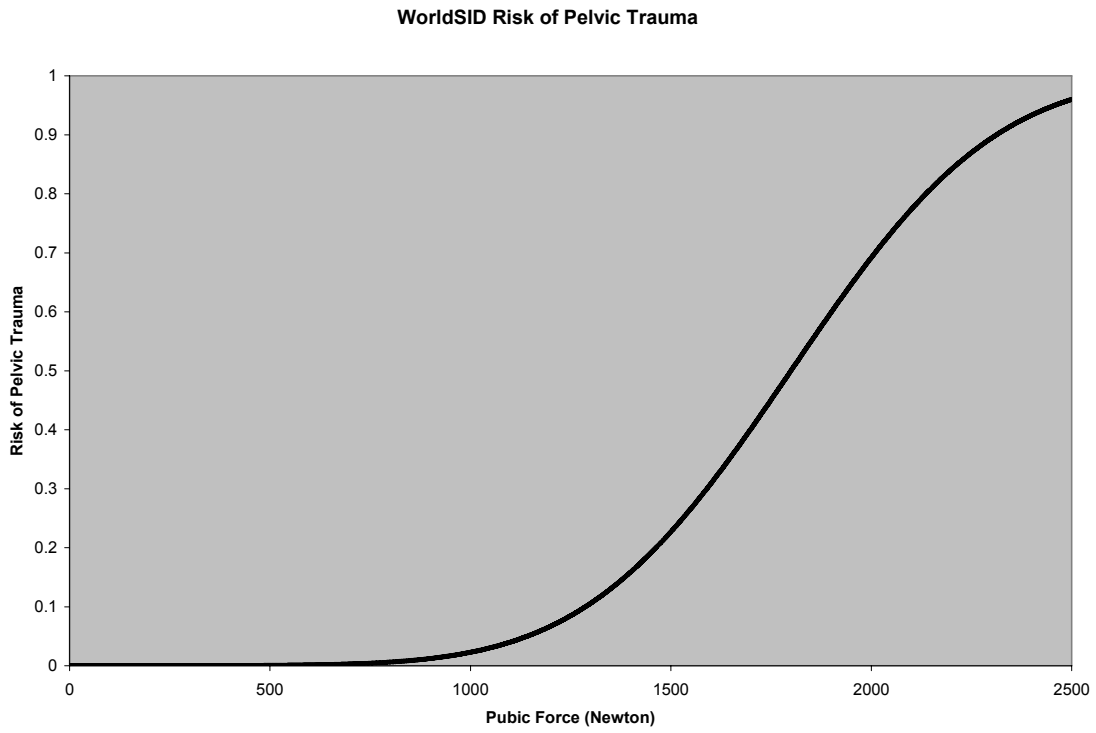

Figure 34 Pubic force

5.7 Limits for the Spine

While all is not know with respect to the failure properties of the spine and there are many methods of testing, the following provides a first order approximation for thoracolumbar injury criteria. Allowable limits for the thoracolumbar spine were developed based on the failure properties reported from all three of the areas of spinal failure property research, (Table 2). The suggested criteria was determined by averaging the failure data, rounded to the nearest hundredth, of predominantly young male cadavers tested at static to semi dynamic rates. Therefore, the suggested criteria can be used for testing with the 50th Percentile male dummy. If there was insufficient data for certain regions in a specific testing mode, then the criteria was scaled based on the averages reported for compression testing because it was the most complete data set. Allowable limits are suggested for the upper thorax, middle thorax, and lumbar regions because these regions correspond to the locations of spinal load cells in the 50th Percentile male dummy.

Table 10 Allowable limits to be closely monitored for the spine

Site in Spine	Pure Compression (N)	Pure Tension (N)	Pure Shear (N)	Combined Compression/ Moment
Upper Thoracic	3100	800	900	100 N-m (@ 1400 N)
Middle Thoracic	4500	1600	1300	146 N-m (@ 2000 N)
Lumbar	6200	220	1800	200 N-m (@ 2430 N)

6 REFERENCES

Bolte, J.H., Hines, M.H. *et al.* (2000). Shoulder response characteristics and injury due to lateral glenohumeral joint impacts. 44th Stapp.

Brown, T., *et al.* (1957). Some mechanical tests on the lumbosacral spine with particular reference to the intervertebral disks. J. Bone and Joint Surg. 39-A(5), pp: 1135-1164.

Chandler, R.F. and Gowdy, R.V. (1983) "Human Exposure to Impact with Two Point (Lapbelt) and Three Point (Lapbelt: and Diagona1 Shoulder Belt) Restraint Systems." Memorandum No. AAC-119-83-7; Protection and Survival Laboratory, Civil Aeromedical Institute, Mike Monroney Aeronautical Center, Federal Aviation Administration, Oklahoma City, Oklahoma 73125.

Demetropoulos, C, *et al.* (1998). Mechanical properties of the cadaveric and hybrid II Lumbar spines. Proceedings of the 42nd Stapp car crash conference, SAE paper number 983160. pp: 1-10.

Dixon, C.E., "Cortical Impact Models of Brain Injury," Frontiers in Head and Neck Trauma, ISO Press, 1998.

Duma, S, *et al.* (2006). Biomechanical response of the lumbar spine in dynamic compression. biomedical sciences instrumentation symposium. 42, pp: 476-481.

Duma, S., Boggess, B., Bass, C., and Crandall, J., (2003) "Injury Risk Functions for the 5th Percentile Female Upper Extremity," SAE Paper 2003-01-0166.

Duma, S.M., Schreiber, P.H., McMaster, J.D., Crandall, J.R., Bass, C.R., Pilkey, W.D., (1999). "Dynamic Injury Tolerance for Long Bones in the Female Upper Extremity," Journal of Anatomy, Vol. 194, Part 3, pp. 463-71.

Federal Aviation Administration (1996). Dynamic evaluation of seat restraint systems and occupant protection on transportation airplanes. Advisory Circular Number: 25.562-1A.

Gabler, HC. (2004). "Harm and Injury Risk of Far Side Impact – Injury Sources."Presentation to the MUARC/GWU Far Side Impact Meeting.

Gabler, H.C., Digges, K., Fildes, B.N., & Sparke, L. (2005a) : "Side impact injury risk for belted far side passenger vehicle occupants", SAE Paper No. 2005-01-0287.

Gabler, H.C., Digges, K., Fildes, B.N., & Sparke, L. (2005b) : "Side impact injury risk for belted far side passenger vehicle occupants", Proceedings of the ESV Conference, Washington. Gennarelli T, Pintar F, Yoganandan N. (2003) "Biomechanical tolerances for diffuse brain injury and a hypothesis for genotypic variability in response to trauma." Proceedings of the AAAM. Lisbon, Portugal.

Gibson, T., Fildes, B., Deery, H., Sparke, L., Benatos, E., Fitzharris, M. McLean, J., & Vulcan, P. (2000): "Improved side impact protection: A review of injury patterns, injury tolerance and dummy measurement capabilities." Monash University Accident Research Centre Report No. 147.

Gibson, T., Benetatos, E., Newstead, S., and Fildes, B., "Improved Side Impact Protection: The Development of Injury Assessment Functions," Proceedings of the 17th ESV Conference, June 2001.

Gibson T, Benetatos E and Newstead S (2001): "Lateral Injury Assessment Functions for Use with the Biosid.", Monash University Accident Research Centre Report.

Haffner , M., Eppinger, R., Rangarajan, N., Shams, T., Artis, M. and Beach, D. (2001).

Hansson, T, *et al.* (1979). The bone mineral content and ultimate compressive strength of lumbar vertebrae. Spine 5(1), pp: 46-55.

Hutton, W, *et al.* (1979). The compressive strength of lumbar vertebrae, J. Anat, 129(4), pp:753-8.

Foundations and Elements of the NHTSA THOR Alpha ATD Design. Proceedings of the ESV Conference, Amsterdam.

Hautmann, E., Scherer, R., Akiyama, A., Page, M., Xu, L., Kostyniuk, G., Sakurai, M., Bortenschlager, K., Harigae, T. and Tylko, S. (2003): "Updated biofidelity rating of the revised WorldSID prototype dummy", 18th ESV Proceedings, Nagaoya, Japan.

IIHS: "Side Impact Crashworthiness Evaluation: Guidelines for rating injury measures (Version II)", IIHS, April 2004.

ISO TC 22/SC 12/WG6 N 613, "Road Vehicles – Injury Risk Curves to Evaluate Occupant Protection in Side Impact," 29 March 2005.

ISO/TC22/SC12/WG6, (2004): "WorldSID injury risk curves." Document N602 prepared by LAB.

ISO/TC22/SC12/WG6 (1999) Document N: Draft Technical Report (DTR-7861) Road Vehicle-Injury Risk Curves to Evaluate Occupant Protection in Simulated Frontal Collisions.

ISO/TR 9790 (1999): Road Vehicles – Anthropomorphic side impact dummy – Lateral impact response requirements to assess the biofidelity of the dummy.

Ivarsson J, Lessley D, Kerrigan J, Bhalla K, Bose D, Crandall J, and Kent R (2004): "Dynamic Response Corridors and Injury Thresholds of the Pedestrian Lower Extremities" IRCOBI.

Kazarian, L and Graves, G (1977). Compressive strength characteristics of the human vertebrae centrum. Spine 2(1), pp: 1-14.

Kennedy, E.A., Hurst, W.J., Stitzel, J.D., Cormier, J.M., Hansen, G.A., Smith, E.P., and Duma, S.M., (2004) "Lateral and Posterior Dynamic Bending of the Mid-Shaft Femur: Fracture Risk Curves for the Adult Population," Proceedings of the STAPP Car Crash Conference.

Kerrigan J, Drinkwater D, Kam C, Murphy D, Ivarsson B, Crandall J and Patrie, J (2004): "Tolerance of the Human Leg and Thigh in Dynamic Latero-Medial Bending." Proceedings of the ICRASH Conference.

Kikuchi, Ono and Nakamura (1982): "Human Head Tolerance to Lateral Impact Deduced from Experimental Head Injuries Using Primates." Proceedings of the 1982 ESV Conference.

Konosu A, Issiki T and Tanahashi M (2005): "Development Of A Pedestrian Lower Extremity Protection Car Using A Biofidelic Flexible Pedestrian Legform Impactor." Proceedings of the ICRASH Conference.

Kuppa S (2004): "Injury Criteria for Side impact Dummies." National Highway Traffic Safety Administration, U. S. Department of Transportation Report.

Lund A (2003): "Recommended Procedures for Evaluating Occupant Risk from Deploying Side Airbags." Technical Working Group.

Margulies SS, and Thibault LE, (1992): "A Proposed Tolerance Criterion for Diffuse Axonal Injury in Man," J. Biomech, 25(8) 1992: 917-23.

Meaney D, Thibault L, Gennarelli T. (1994) "Rotational brain injury tolerance criteria as a function of vehicle crash parameters." IRCOBI. Lyon, France.

Morris A, Hassan A, Mackay M, et al. (1993) "Head injuries in lateral impact collisions." Proceedings of IRCOBI.

McLean AJ. (1996) "Brain injury without head impact?" In Bandak FB, Eppinger RH, Ommaya AK eds. *Traumatic Brain Injury.* Larchmount, NY: Mary Ann Liebert Inc.

Mertz H, Irwin A, and Prasad P (2003): "Biomechanical and Scaling Basis for Frontal and Side Impact Injury Assessment Reference Values." Proceedings of the STAPP Car Crash Conference.

Messerer, O (1880). Uber elasticitat and festigkeit der menschlichen knochen. Stuttgart, J.G. Cottaschen Buchhandeling.

MUARC (2003): Worksheet For Task 5 – Test Procedures And Injury Criteria, ARC Far Side Collaborative Research Program,

Myklebust, J (1989). Experimental spinal trauma studies in human and monkey cadavers. Proceedings of the 27th Stapp car crash conference, SAE paper number 831614. pp: 149-161.

Newman JA, Shewchenko N, Welbourne E (2000). "A Proposed New Biomechanical Head Injury Assessment Function - The Maximum Power Index." Proceedings of the 44th Stapp Car Crash Conference.

NHTSA (1995) Final Economic Assessment, FMVSS 201 Upper Interior Head Protection. Office of Regulatory Analysis, Plans and Policy. Washington DC.

Ommaya A (1988). "Mechanisms and Preventative Management of Head Injuries: A Paradigm for Injury Control." The George Snively Memorial Lecture given at the 32nd AAAM.

Ono, K., “Current Status on Human Impact Tolerance, Clinical and Biomechanical,” Frontiers in Head and Neck Trauma, ISO Press, 1998.

Perry, O (1957). Fracture of the vertebral end-plate in the lumbar spine. Acta Orthop. Scad. 25 (suppl.), pp: 2-101.

Pintar, F (1986). The biomechanics of spinal elements. Doctoral Dissertation. Marquette University Graduate School. Milwaukee, WI.

Rouhana, SW, Lau, IV, and Ridella, SA, Influence of Velocity and Forced Compression on the Severity of Abdominal Injury in Blunt Non-penetrating Lateral Impact, J. Trauma, Vol. 25(6): 490 – 500, 1985.

SAE (1980), ‘Human tolerance to impact conditions as related to motor vehicle design’, SAE Information Report no. SAE J885 APR80, Society of Automotive Engineers, Warrendale, PA.

Scherer R, Cesari D, Uchimura T, Kostyniuk G, Page M, Asakawa K, Hautmann E, Bortenschlager K, Sakurai M and Harigae T (2001): “Design And Evaluation Of The Worldsid Prototype Dummy.” ESV.

Sonoda, T (1962). Studies on the strength for compression, tension, and torsion of human vertebrae column. J. Kyoto Pref. Med. Univ. 71, pp: 659-702.

Sundararajan, S (2005). Characteristics of PMHS lumbar motion segments in lateral shear. Proceedings of the 49th Stapp car crash conference, pp: 367-379.

Yoganandan, N, Pintar, FA, Zhang, Gennarelli, TA and Beuse, N, (2005) “Biomechanical Aspects of Blunt and Penetrating Head Injuries.” Proceedings of the IUTAM Conference.

Yoganandan, N, *et al.* (1989). Stiffness and strain energy criteria to evaluate the threshold of injury to an intervertebral joint. J. Biomechanics 22, pp: 135-142.

Yoganandan, N, *et al.* (1988). Biomechanical investigations of the human thoracolumbar spine. SAE technical paper number 881331. pp: 1-9.

Zaborowski, A (1966). “Lateral Impact Studies – Lap Belt Shoulder Harness Investigation.” Proceedings of the Stapp Car Crash Conference.

7 ACKNOWLEDGEMENT

The funding for this research has been provided [in part] by private parties, who have selected Dr. Kennerly Digges [and FHWA/NHTSA National Crash Analysis Center at the George Washington University] to be an independent solicitor of and funder for research in motor vehicle safety, and to be one of the peer reviewers for the research projects and reports. Neither of the private parties have determined the allocation of funds or had any influence on the content of this report.

The Australian Research Council awarded Grant No. LP0454122 to Professor Brian Fildes at the Monash University Accident Research Centre. The Australian Research Council has not determined the allocation of funds or had any influence on the content of this report.

Publication and technical editing were performed by Morgan Consulting.